

ECCENTRICALLY BRACED STEEL FRAMES AS A SEISMIC FORCE RESISTING
SYSTEM

by

SAMUEL DALTON HAGUE

B.S., Kansas State University, 2013

A REPORT

submitted in partial fulfillment of the requirements for the degree

MASTER OF SCIENCE

Department of Architectural Engineering
College of Engineering

KANSAS STATE UNIVERSITY
Manhattan, Kansas

2013

Approved by:

Major Professor
Kimberly Waggle Kramer, P.E., S.E.

Copyright

SAMUEL DALTON HAGUE

2012

Abstract

Braced frames are a common seismic lateral force resisting system used in steel structure. Eccentrically braced frames (EBFs) are a relatively new lateral force resisting system developed to resist seismic events in a predictable manner. Properly designed and detailed EBFs behave in a ductile manner through shear or flexural yielding of a link element. The link is created through brace eccentricity with either the column centerlines or the beam midpoint. The ductile yielding produces wide, balanced hysteresis loops, indicating excellent energy dissipation, which is required for high seismic events.

This report explains the underlying research of the behavior of EBFs and details the seismic specification used in design. The design process of an EBF is described in detail with design calculations for a 2- and 5-story structure. The design process is from the AISC 341-10 *Seismic Provisions for Structural Steel Buildings* with the gravity and lateral loads calculated according to ASCE 7-10 *Minimum Design Loads for Buildings and Other Structures*. Seismic loads are calculated using the Equivalent Lateral Force Procedure. The final member sizes of the 2-story EBF are compared to the results of a study by Eric Grusenmeyer (2012). The results of the parametric study are discussed in detail.

Table of Contents

List of Figures	vi
List of Tables	vii
Acknowledgements	viii
Dedication	ix
Notations	x
Chapter 1 - Introduction	1
Chapter 2 - Seismic Forces and Building Interaction	3
Ground Motion	3
Seismic Forces in Load Combinations	4
Application of Seismic Force	6
Seismic Base Shear	7
Seismic Design Category	7
Response Modification Coefficient	10
Seismic Response Coefficient	11
Effective Seismic Weight	12
Vertical Distribution of Seismic Force	13
Horizontal Distribution of Seismic Force	14
Chapter 3 - Eccentric Brace Frames	15
Link Length and Behavior	16
Theoretical Links	17
Strain Hardening	18
Shear Links	19
Intermediate Links	19
Flexure Links	20
Link Rotation and Stiffness	21
Link Connections	23
Chapter 4 - Design of Eccentric Brace Frame	25
Link Design	25
Shear Strength	25

Link Length.....	26
Rotation Angle	27
Stiffeners	28
Bracing.....	29
Beam Design.....	30
Brace Design.....	31
Column Design	32
Connections	33
Demand Critical Welds.....	33
Beam-to-Column Connections.....	33
Brace Connections	34
Elastic and Inelastic Drift Considerations	34
Second-Order Analysis.....	35
The B_1 Multiplier	36
The B_2 Multiplier	37
Chapter 5 - Parametric Study	38
Parametric Study Overview	38
Governing Lateral Load.....	41
Results.....	41
Member Sizes.....	42
Story Drift	44
Second-Order Effects.....	45
Special Concentrically Braced Frames Comparison.....	47
Conclusions.....	49
References.....	51
Bibliography	53
Appendix A – Load Calculations.....	56
Appendix B – Load Combinations	64
Appendix C – EBF Member Design.....	74

List of Figures

Figure 1-1: Elevation of EBF and CBF	1
Figure 2-1: Lateral Force-Displacement and Overstrengths of a Brittle System.....	6
Figure 2-2: Inelastic Force-Deformation Curve of a Ductile System.....	11
Figure 3-1: Eccentric Brace Frame Configurations	16
Figure 3-2: Static Equilibrium of Link Element	17
Figure 3-3: Idealized Structural Steel Stress-Strain Curve	18
Figure 3-4: Link Rotation Demand.....	22
Figure 3-5: Link-to-Column Moment Distribution.....	23
Figure 4-1: Link Rotation Angle.....	28
Figure 4-2: EBF with Interior Eccentric Brace.....	32
Figure 4-3: P-Delta Effects	35
Figure 5-1: Building Framing Plan	39
Figure 5-2: Five-Story Transverse Elevation.....	40

List of Tables

Table 2-1: Site Classification and Soil Type	9
Table 2-2: Simplified Risk Categories.....	10
Table 5-1: Base Shear Comparison.....	41
Table 5-2: 2-Story Member Results.....	43
Table 5-3: 5-Story Member Results.....	44
Table 5-4: Interstory Drift by Level.....	45
Table 5-5: Interstory Drift Summary	45
Table 5-6: Second Order Factors for 2- and 5-story Frames	46
Table 5-7: Comparison of Two-Story EBF and SCBF (Grusenmeyer, 2012) Results.....	48

Acknowledgements

I would like to thank my major professor, Kimberly Kramer, P.E., S.E., who pushed me out of my comfort zone for my own good. Thank you also to my committee members, Jim Goddard, and Charles Burton, P.E. I would also like to thank all of my previous teachers and professors who helped me realize my full potential throughout my educational career.

Dedication

This report is dedicated to my parents, Mike Hague and Kathy Williams for their unwavering support and encouragement.

Notations

A_{lw}	=	Link Web Area
B_1	=	Multiplier to Account for P- δ Effects
B_2	=	Multiplier to Account for P- Δ Effects
b_f	=	Flange Width
C_d	=	Drift Amplification Factor
C_m	=	Curvature Constant
C_s	=	Seismic Response Coefficient
C_{vx}	=	Vertical Distribution Factor
D	=	Dead Load
e	=	Link Length or Eccentricity
E	=	Modulus of Elasticity
F_a	=	Site Coefficient for a 0.2 Second Period
F_v	=	Site Coefficient for a 1 Second Period
F_x	=	Lateral Seismic Force at Level 'x'
F_y	=	Specified Minimum Yield Stress
h	=	Frame Height
H	=	Story Shear
h_o	=	Distance Between Flange Centroids
h_x	=	Height from Base of Structure to Level 'x'
I	=	Moment of Inertia
I_e	=	Seismic Importance Factor
k	=	Structural Period Modification Factor
K_e	=	Effective Length Factor
L	=	Live Load
L	=	Length
L_b	=	Unbraced Length
MCE	=	Maximum Considered Earthquake Response Spectrum
MCE_R	=	Risk-Targeted Maximum Considered Earthquake Response Spectrum
M_p	=	Plastic Moment
P_{el}	=	Elastic Critical Buckling Strength
P_{estory}	=	Elastic Critical Buckling Strength for the Story
P_{mf}	=	Total Vertical Load in Moment Frame Columns
P_{story}	=	Total Vertical Load Supported by the Story
P_u	=	Required Axial Strength
P_y	=	Nominal Axial Yield Strength
Q_E	=	Horizontal Seismic Force
R	=	Response Modification Coefficient
R_y	=	Ratio of Expected Yield Stress to Specified Minimum Yield Stress

S	=	Snow Load
S_1	=	Mapped MCE Spectral Response Acceleration for a 1 Second Period
S_{D1}	=	Design Spectral Response Acceleration Parameter for a 1 Second Period
S_{DS}	=	Design Spectral Response Acceleration Parameter for a 0.2 Second Period
S_{M1}	=	MCER Spectral Response Acceleration Parameter for a 1 Second Period
S_{MS}	=	MCER Spectral Response Acceleration Parameter for a 0.2 Second Period
S_S	=	Mapped MCE Spectral Response Acceleration for a 0.2 Second Period
t_w	=	Web Thickness
U_{lt}	=	First-Order Moment or Axial force using Load Combinations due to Lateral Translation of the Structure Only
U_{nt}	=	First-Order Moment or Axial force using Load Combinations with the Structure Restrained Against Lateral Translation
U_r	=	Required Second-Order Moment or Axial Strength
V	=	Design Base Shear
V_E	=	Elastic Lateral Force
V_n	=	Nominal Shear Strength
V_p	=	Plastic Shear
V_S	=	Design Lateral Force
V_Y	=	Lateral Force at Yield
W	=	Effective Seismic Weight
w_x	=	Portion of Total Effective Seismic Weight at Level 'x'
Z	=	Plastic Section Modulus
α	=	ASD/LRFD Adjustment Factor
β_{br}	=	Required Brace Stiffness
γ_p	=	Plastic Link Rotation Angle
Δ_a	=	Allowable Story Drift
Δ_H	=	First-Order Interstory Drift Resulting from Story Shear, H
Δ_p	=	Plastic Story Drift
δ_x	=	Amplified Deflection at Level 'x'
δ_{xe}	=	Elastic Lateral Displacement at Level 'x'
δ_{xie}	=	Inelastic Lateral Displacement at Level 'x'
Θ_p	=	Plastic Story Drift Angle
ϵ	=	Strain
ρ	=	Redundancy Factor
ρ_o	=	Link Length Ratio
ϕ	=	Strength Reduction/Resistance Factor
σ	=	Stress
Ω_0	=	Overstrength Factor
Ω_D	=	Design Overstrength
Ω_M	=	Material Overstrength
Ω_S	=	System Overstrength

Chapter 1 - Introduction

Following extensive research in the 1970s, '80s, and '90s, Eccentrically Braced Frames (EBFs) have become a widely accepted form of seismic force resisting system. Prior to this research, EBFs had been an accepted form of wind bracing (Popov & Engelhardt, 1988). An EBF is a brace frame system in which one end of the brace is connected to the beam instead of a frame node, shown as black circles, as in concentrically braced frames (CBFs). Figure 1-1 illustrates the differences between the member configuration and nodes of a CBF and an EBF. Figure 1-1a depicts an EBF where the longitudinal axis of each brace has an eccentricity to the midpoint of the beam equal to one-half the link length. Figure 1-1b, depicts a CBF in the chevron configuration where the longitudinal axis of each brace intersects at the midpoint of the beam.

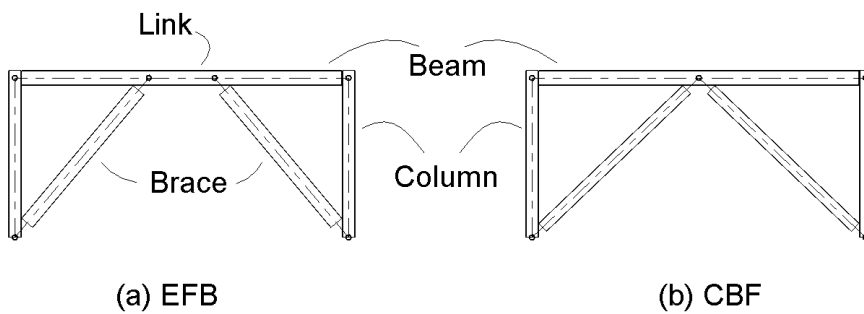


Figure 1-1: Elevation of EBF and CBF

The length of beam between the brace and the frame node is known as a link. Brace forces are introduced to the frame through shear and flexure in the link, so the link acts as a seismic fuse.

This report examines the design process of EBFs through a detailed analysis of each frame component and through a parametric study of two hypothetical buildings with the same framing plan of varying heights subjected to wind and seismic lateral loads. Gravity and lateral loads per the 2012 *International Building Code* are determined using ASCE 7-10 *Minimum Design Loads for Buildings and Other Structures*. Additionally, the maximum feasible building height for the proposed building exposed to equivalent lateral forces using the approximate

second-order analysis per AISC 360-10 is examined; to illustrate the importance of second-order effects, each building is analyzed with and without second-order effects.

The most common method for applying seismic loads to a structure similar to the buildings in this parametric study is the equivalent lateral force procedure (ELFP). In designing a SFRS, it is important to understand the EFLP, which converts a dynamic seismic event into a linear, static event, and how this linear force is applied to a building. Beyond understanding the loading procedure, it is important to understand how forces are transferred internally between members and how the SFRS dissipates energy. As such, Chapter 2 outlines the design process of the ELFP; further, Chapter 2 illustrates how the forces determined from the ELFP are distributed vertically and horizontally to the structure.

Once the lateral forces are distributed throughout the structure, they must be resisted and dissipated. Chapter 3 discusses the behavior of an EBF and follows with an in-depth look into the behavior of the seismic fuse of an EBF: the link.

The results of theoretical, behavioral analyses are practical design methods; as such, Chapter 4 examines the design requirements for each component of an EBF to ensure the behavior of each component and the overall structure fits the desired model. To provide context to the design requirements, Chapter 5 contains the results and conclusions of a parametric study of a hypothetical structure in Memphis, Tennessee. The structure is 120'-0" by 75'-0" consisting of 4 bays of 30'-0" and 3 bays of 25'-0", respectively; each principle direction has 4 LRFS frames at the exterior of the building. The design of EBFs includes calculating the seismic force imposed on a building, determining the resulting forces within seismic force resisting system (SFRS), and then sizing frame members based on the resulting forces. To provide a point of reference to the results of this study, a comparison between the results of this study and of a previous study by Eric Grusenmeyer (2012) of CBFs is included. Design calculations are presented for this study.

Chapter 2 - Seismic Forces and Building Interaction

This chapter focuses on how seismic forces are determined and applied to buildings. The seismic forces for designing structures are determined using current seismic code provisions. The governing building code is the *2012 International Building Code* (IBC). The IBC prescribes the American Society of Civil Engineers ASCE/SEI 7-10 *Minimum Design Loads for Buildings and Other Structures* (ASCE 7) to determine loads on buildings.

The ASCE 7 requires structures to resist maximum considered earthquake (MCE) ground motions instead of earthquake magnitudes. MCE ground motions are based on the relative frequency and distribution of earthquakes of specific regions. By designing a structure to resist a MCE ground motion, the design approaches presented in the ASCE 7 provide a relatively uniform margin of safety against collapse across the United States, which could not be as effectively achieved through designing for earthquake magnitudes (Leyendecker, Hunt, Frankel, & Rukstales, 2000).

Ground Motion

Seismic events impose dynamic loading on a building, as the ground acceleration during an event occurs in a cyclic pattern. To simplify seismic design, ASCE 7 allows the use of the ELFP for buildings meeting certain requirements. The ELFP yields a static force based on local ground accelerations.

MCE ground motions are defined as the maximum level of seismic ground acceleration that is considered as reasonable to design typical low-rise structures without severe structural irregularities to resist. As such, the ASCE 7 uses a uniform probability of exceedance of 2% in 50 years, which is a return period of approximately 2500 years. Ground motions can exceed MCE values, but it was deemed economically impractical to design normal structures to higher levels of seismic resistivity (Leyendecker, Hunt, Frankel, & Rukstales, 2000). Within the ASCE 7, the 2% exceedance in 50 year accelerations are called mapped MCE spectral response acceleration parameters. To simplify the design process in the ELFP, the mapped MCE spectral response accelerations are presented short period of 0.2 seconds and a long period of 1.0 second, which relate to the period of a rigid and flexible building, respectively.

Radiating from the epicenter, seismic waves propagate through the layers of the earth to the crust. Seismic waves travel through the layers of the earth at a rate that is dependent on the composition of each layer. By measuring the interference of shear-wave velocities, the amplification or dampening of ground motions can be estimated. As soil stiffness increases, soil shear-wave velocity increases; furthermore, as soil shear-wave velocity increases, ground motion amplification decreases. To summarize, a site with stiff soil or rock will experience a lower level of ground motion amplification than a site with soft soil or clay (Building Seismic Safety Council, 2004). ASCE 7 presents mapped MCE spectral response acceleration parameters normalized for one site class; therefore, mapped MCE spectral response acceleration parameters must be modified to correspond to site-specific conditions. A MCE response spectrum that has been modified for site conditions is referred to as a Risk-Targeted Maximum Considered Earthquake (MCE_R) response spectrum.

To attain design level ground motions, MCE_R spectral response acceleration parameters are divided by a factor of 1.5, which is the lower bound for estimates of the margin against collapse. The lower bound factor is represented as 2/3 in ASCE 7 (Leyendecker, Hunt, Frankel, & Rukstales, 2000).

Seismic Forces in Load Combinations

Structures must resist a combination of various gravity and environmental loads. The governing combinations for a structure are given in Chapter 2 of the ASCE 7; the load combinations for Load and Resistance Factor Design (LRFD) presented in ASCE 7 Section 2.3.2 of the ASCE 7 require expansion for the design of SFRS. The modifications not only separate the seismic load into horizontal and vertical components, but also establish adequate redundancy and overstrength in SFRS components. Redundancy and overstrength modifications are found in ASCE 7 Section 12.4.2.3 and 12.4.3.2, respectively.

The LRFD modified load combinations of Section 12.4.2.3 are as follows:

$$5. (1.2 + 0.2S_{DS})D + \rho Q_E + L + 0.2S \quad (\text{Equation 2-1})$$

$$7. (0.9 - 0.2S_{DS})D + \rho Q_E \quad (\text{Equation 2-2})$$

These modified load combinations include ρ , the redundancy factor; $0.2S_{DS}$, a dead load factor for the vertical component of a seismic load; and Q_E , the horizontal seismic force (V). The redundancy factor reduces the response modification coefficient, R , for less redundant structures, which increases the applied seismic load. This introduces an incentive to design structures with well-distributed SFRS, meaning multiple load paths exist for a give force. Conditions where the redundancy factor can be taken as unity are presented in ASCE 7 Sections 12.3.4.1 and 12.3.4.2 of ASCE 7.

The LRFD modified load combinations of Section 1.4.3.2 are:

$$5. (1.2 + 0.2S_{DS})D + \Omega_o Q_E + L + 0.2S \quad (\text{Equation 2-3})$$

$$7. (0.9 - 0.2S_{DS})D + \Omega_o Q_E \quad (\text{Equation 2-4})$$

These modified load combinations include Ω_o , the overstrength factor and the previously discussed $0.2S_{DS}$ and Q_E . The overstrength factor is intended to take into consideration situations where failure of an isolated, individual, brittle element results in the loss of an entire SFRS or in instability leading to collapse. The overstrength factor is the ratio of the maximum force to the plastic strength, as shown in Figure 2-1, and is a combination of three separate overstrengths inherent within a SFRS: design overstrength (Ω_D), material overstrength (Ω_M), and system overstrength (Ω_S).

Design overstrength, represented by Point 1 in Figure 2-1, is the difference between the lateral force as first yield and the minimum design strength force. Systems that are strength controlled, such as CBF, tend to have lower design overstrength. Conversely, systems that are drift controlled, such as MRF, tend to have higher design overstrength. In other words, design overstrength exists when members' strengths are increased from minimum required values to combat drift or deflection.

Material overstrength, represented by the difference between Points 1 and 2 in Figure 2-1, is a result of conservatism in design values that are based on lower bound estimates of actual strengths.

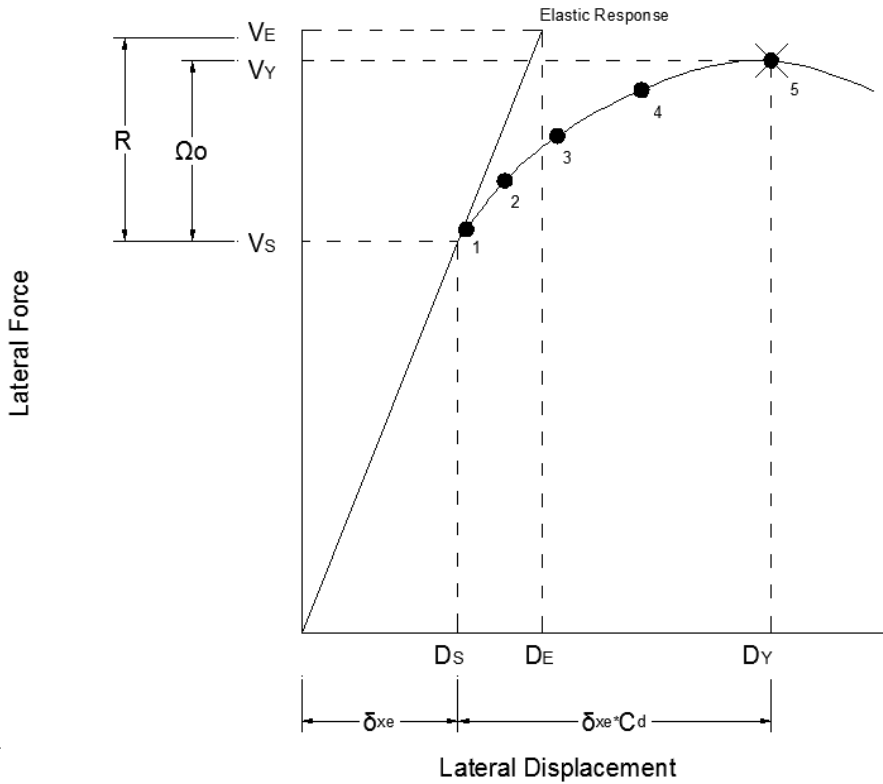


Figure 2-1: Lateral Force-Displacement and Overstrengths of a Brittle System

System overstrength, represented by the difference between Points 2 and 5 in Figure 2-1, is a result of redundancy within a structural system. Points 3 and 4 represent major yields within the structure before overall failure. Rather, system overstrength is the difference between the maximum force a structure is capable of resisting and the force at first yield. For example, a single story, single bay structure has a system overstrength of unity, as first yield results in a fully yielded system (Building Seismic Safety Council, 2004).

As seismic forces must be carried through a structural system before dissipated by the SFRS, the modified load combinations are to be used in the design of all structural members not just the SFRS.

Application of Seismic Force

The ASCE 7 has three permitted analytical procedures. The ELFP, which is the method used in this report, is outlined in ASCE 7 Section 12.8. The ELFP takes the dynamic load of an earthquake and applies the load statically to the structure; the structure is rigid enough and the

seismic force's rate of application is slow enough such that the first mode of movement is the governing case for the design of the structure. The provisions also permit a Modal Response Spectrum Analysis in ASCE 7 Section 12.9, and a Seismic Response History Procedure in ASCE 7 Chapter 16. Both the Modal Response Spectrum Analysis and the Seismic Response History Procedure are dynamic analysis procedures. Furthermore, the ELFP has a simplified approach that is permissible if all of the conditions of ASCE 7 Section 12.14 are met. ASCE 7 Table 12.6-1 outlines the permissibility requirements for the three main analytical procedures.

ASCE 7 Section 12.8 outlines the ELFP. To begin, the seismic base shear is determined. The base shear is then vertically distributed to each level based on each level's effective seismic weight and height above the base. The distributed lateral force is then imposed at each level's center of mass about each level's center of rigidity using seismic load combinations where it is transmitted to the SFRS to be dissipated.

Seismic Base Shear

The ELFP is a first mode application of the modal response spectrum analysis in which all of the structure's mass is active in the first mode. A static force equivalent to the dynamic forces of a seismic event is applied to a structure. The equivalent force is calculated using ASCE 7 Equation 12.8-1, shown.

$$V = C_s W \quad \text{(Equation 2-5)}$$

where

V = seismic base shear

C_s = seismic response coefficient

W = effective seismic weight

The base shear is applied to the structure using the orthogonal combination procedure outlined in ASCE 7 Section 12.5.3, which states that design seismic forces are to be applied independently in any two orthogonal directions. Additional loading requirements for a structure in Seismic Design Category (SDC) C and greater are outlined in ASCE 7 Section 12.5.3 and 12.5.4.

Seismic Design Category

The SDC is a classification, ranging from A to F with A being the lowest seismic event, applied to structures based upon site ground accelerations and soil conditions and building use with categories. Once the SDC is established, many design requirements, such as height limits and detailing requirements, can be determined. Furthermore, the calculations required to determine the SDC provide useful values related to ground motion.

To determine the SDC, the mapped MCE spectral response acceleration parameters, S_S and S_1 , are modified to fit site soil conditions and to reflect lower bound values. S_S and S_1 are normalized to Site Class B, so they must be modified for the soil type at the building location. ASCE 7 Equations 11.4-1 and 11.4-2, shown below, determine the mapped MCE_R spectral response acceleration parameters, which are adjusted for site soil conditions.

$$S_{MS} = F_a S_S \quad \text{(Equation 2-6)}$$

$$S_{M1} = F_v S_1 \quad \text{(Equation 2-7)}$$

where

S_{MS} and S_{M1} = MCE_R spectral response acceleration parameter for a 0.2 second and a 1 second period, respectively

F_a and F_v = site coefficients for a 0.2 second and a 1 second period, respectively

S_S and S_1 = mapped MCE spectral response accelerations for a 0.2 second and a 1 second period, respectively

Mapped MCE spectral response accelerations S_S and S_1 are found in ASCE 7 Figures 22-1 to 22-6. Low-rise structures are generalized in the ELFP as having a period of 0.2 seconds while mid-rise to high-rise structures are generalized to 1 second. Structures with periods greater than 1 second are typically analyzed using dynamic procedures. The different Site Classes are shown in Table 2-1. The coefficients F_a and F_v are determined from ASCE 7 Tables 14.4-1 and 14.4-2, respectively.

Table 2-1: Site Classification and Soil Type

Site Class	Soil Type
A	Hard Rock
B	Rock
C	Very Dense Soil and Soft Rock
D	Stiff Soil
E	Soft Clay Soil
F	Site Response Analysis Required

Soil conditions greatly affect the propagation and amplification of seismic waves. For soft soils with a low shear modulus, there is higher amplification than in stiff soils with a high shear modulus. Additionally, long period waves are typically amplified greater than short period waves. For that reason, mapped MCE spectral response accelerations have separate site coefficient factors. The coefficients in ASCE 7 Table 14.4-1 and 14.4-2 reflect the amplification of the ground motion expected during a maximum considered earthquake based on observations from the 1989 Loma Prieta earthquake (Building Seismic Safety Council, 2004).

The MCE_R spectral response acceleration parameters are adjusted to fit the lower bound for estimates of the margin against collapse, as discussed previously. These adjusted values are the design spectral response acceleration parameters S_{DS} for short periods and S_{D1} for a period of 1 second. The S_{DS} and S_{D1} parameters are determined by ASCE 7 Equations 14.4-3 and 14.4-4, respectively:

$$S_{DS} = \frac{2}{3} S_{MS} \quad (\text{Equation 2-8})$$

$$S_{D1} = \frac{2}{3} S_{M1} \quad (\text{Equation 2-9})$$

where

S_{DS} and S_{D1} = design spectral response acceleration parameters for a 0.2 second period and a 1 second period, respectively

The Risk Category of a building is based on the risk to the health, safety, and welfare of the public if the building is damaged. Risk Categories range from I to IV with I being the lowest

risk and are outlined in ASCE 7 Table 1.5-1. Each Risk Category has an associated importance factor found in ASCE Table 1.5-2. A simplified interpretation of Risk Categories is shown in Table 2-2. The Risk Category and the design spectral response acceleration parameters are what determine the SDC. Each acceleration parameter is assigned to a SDC and the parameter with the highest alpha-order category is the governing category for the building. The SDCs based on short periods and a 1-second period are determined using ASCE 7 Table 11.6-1 and 11.6-2, respectively. Provisions for categories E and F, as well as requirements for a simplified procedure, are outlined in Section 11.6.

Table 2-2: Simplified Risk Categories

Risk Category	Failure of Building Represents
I	Low risk to human life
II	All other buildings
III	Substantial risk to human life
IV	Substantial hazard to the community

Response Modification Coefficient

The response modification coefficient, R , accounts for the damping, overstrength, and ductility intrinsic to elements within a structure. As a ratio of the elastic structural response to the design structural response, the response modification coefficient is always greater than unity. Figure 2-2, shows the inelastic force-deformation curve for a ductile system, which illustrates the relationship between lateral seismic force and deformation.

Structures first respond elastically to lateral forces. Elastic behavior is followed by inelastic behavior caused by the formation of plastic hinges throughout the structure, which are indicated by black circles on the deformation curve. Plastic hinge formation eventually culminates in a yield mechanism, which corresponds to the fully yield strength, V_Y . Brittle structures with low ductility cannot tolerate significant deformation beyond the initial yield; therefore, the inelastic curve does deviate much from the elastic response curve. As a result, the elastic seismic force demand, V_E , is close to that of the fully yielded strength, thereby reducing the response modification coefficient. For comparison, a brittle force-deformation curve is shown in in Figure 2-1. Highly ductile structures can withstand large amounts of deformation

beyond the initial yield, which flattens the inelastic force-deformation curve thereby increasing the response modification coefficient (Building Sesimic Safety Council, 2004).

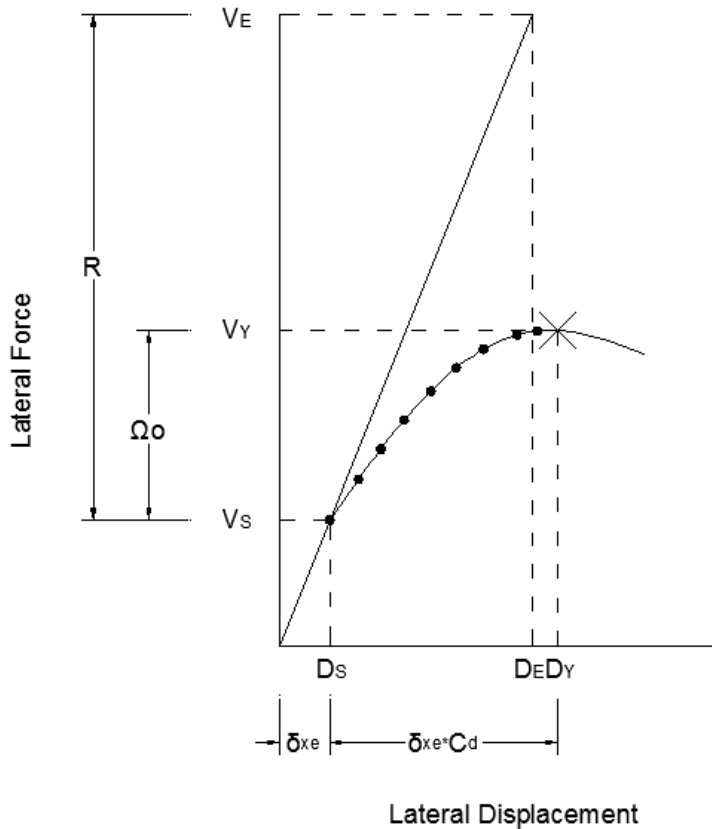


Figure 2-2: Inelastic Force-Deformation Curve of a Ductile System

The response modification coefficient is based on the type of vertical seismic force resisting system a building utilizes. The inelastic force-deformation curve, which provides the response modification coefficient, can be determined through testing or nonlinear static (pushover) analysis. In ASCE 7, R -values for SFRSs are given in Table 12.2-1.

Seismic Response Coefficient

The seismic response coefficient, C_s , is the acceleration imparted into a structure as a percentage of gravitational force. Determined by ASCE 7 Equation 12.8-2, the seismic response coefficient is a factor of the seismicity of the site, the ductility of lateral system, and occupancy category of the structure.

$$C_s = S_{DS} / (R/I_e) \quad \text{(Equation 2-10)}$$

where

C_s = seismic response coefficient

S_{DS} = design spectral response acceleration parameter for short periods

R = response modification coefficient

I_e = seismic importance factor

The seismic importance factor appears in this equation to reduce the response modification coefficient. As structures enter the inelastic range, sizable and permanent deformation occurs that causes damage to the structure. For structures deemed vital to the community or a hazardous upon failure, a limited amount of inelastic deformation is desired (Building Seismic Safety Council, 2004). Minimum values for the seismic response coefficient are determined using ASCE 7 Equations 12.8-3 and 12.8-4 while minimum values are determined using Equations 12.8-5 and 12.8-6.

Effective Seismic Weight

The effective seismic weight of a structure, W , is the total dead load of the structure plus five additional loads outlined in ASCE 7 Section 12.7.2. The additional loads are those that have a high likelihood of being present during a seismic event, but are not included in the structural dead load. The first load applies to storage areas, stating that 25 percent of the floor live load must be included. This load is included because in areas designated as storage, there is a strong likelihood the stored material will be present during a seismic event.

The second load applies to moveable partitions; moveable partitions are partitions that can be moved over the life of the structure, such as, cold-formed steel studs with gypsum board. The greater of the actual weight of the partitions and a minimum of 10 psf over the floor area in question is included in the seismic weight. While moveable partitions are a portion of floor live load when designing for gravity members, they are included in the seismic weight because while they are movable, they are typically present throughout the life of the structure.

The third load applies to permanent equipment. Equipment related to the buildings mechanical, electrical, and plumbing systems that is not calculated into the total dead load, such as a cooling tower, is to be included in the seismic weight.

The fourth load applies to the buildings flat roof snow load. Regions where the flat roof snow load exceeds 30 psf must include 20 percent of the uniform design snow load for all roof slopes. Only a portion of the snow load is required as the likelihood of an extreme snow event and an extreme seismic event occurring simultaneously is low. Flat roof snow loads of less than 30 psf are negligible for that reason.

The final load applies to roof gardens and similar areas. If a building supports landscaping and other similar materials above grade, the total weight of those materials must be included in the seismic weight.

The effective seismic weight is the combination of the dead load of the structure and the five other loads previously described. For ease of overall calculation, the effective seismic weight is determined at each floor level, which is used in the vertical distribution of seismic base shear, and then combined into a total building weight.

Vertical Distribution of Seismic Force

Once the base shear has been calculated, it is vertically distributed to the structure according to ASCE 7 Section 12.8.3. The total base shear is divided into concentrated lateral seismic loads applied at each level. As the ELFP assumes the first mode of movement controls the design, all distributed forces are applied in the direction of the total equivalent force. The proportion of total base shear applied a level is related to the effective seismic weight and the height of the level in question. Equations 12.8-11 and 12.8-12 of ASCE 7 Section 12.8.3 calculate the lateral seismic force induced at any level and the vertical distribution factor for said level, respectively.

$$F_x = C_{vx}V \quad \text{(Equation 2-11)}$$

where

F_x = lateral seismic force at level x

C_{vx} = vertical distribution factor for level x

V = total design base shear

$$C_{vx} = w_x h_x^k / \sum_{i=1}^n (w_i h_i^k) \quad (\text{Equation 2-12})$$

where

w_i and w_x = portion of total effective seismic weight at level i or x

h_i and h_x = the height from the base to level i or x

k = structural period modification factor

Horizontal Distribution of Seismic Force

After the seismic base shear is vertically distributed to each level, the load must be horizontally distributed through the diaphragm. The load is horizontally distributed based on the rigidity of the diaphragm. If the diaphragm is flexible, the force is transmitted based on tributary area. If, however, the diaphragm is rigid, the force is transmitted based on the lateral stiffness of the vertical resisting elements, which introduces inherent and accidental torsional moments outlined in ASCE 7 Sections 12.8.4.1 and 12.8.4.2, respectively.

Chapter 3 - Eccentric Brace Frames

Moment Resisting Frames (MRF) and Concentrically Braced Frames (CBF) are the most commonly utilized systems of the LFRSs permitted in ANSI/AISC 341-10 *Seismic Provisions for Structural Steel Building* (AISC 341). MRFs have a high level of ductility, making them an excellent option to dissipate energy for high seismic events, such as those that occur when a structure is in SCD D, E, or F. However, the high level of ductility comes at a cost: a low level of lateral stiffness. MRFs have a lower level of lateral stiffness than CBFs since they lack braces, and the low lateral stiffness of MRFs can cause story drift at levels exceeding drift limitations. As such, MRFs are designed around drift instead of strength, resulting in reduced economy. Conversely, CBFs have a high level of lateral stiffness and a low level of ductility. For CBFs to be utilized in high seismic regions, special detailing is required to ensure that the frames behave in the prescribed manner. In the 1970s, a new set of frame configurations, shown in Figure 3-1, was proposed for seismic design that would combine the advantages of MRFs and CBFs while decreasing the disadvantages; the seismic-resisting EBF is the product of decades of research. Figure 3-1a depicts a modified chevron configuration in which there is one mid-beam link per level; the braces of the above level could be inverted to form a modified two-story X configuration, which would reduce the axial load transferred to the beams. The frame configuration in Figure 3-1b depicts a column-link configuration in which the link is adjacent to one of the frame columns. Figure 3-1c depicts a second modified chevron configuration in which two links are created due to brace-column eccentricity; in this case, one link is considered active and one passive. The passive link can introduce uncertainty in the inelastic behavior of the frame as the two links do not necessarily equally share the inelastic deformation, as the nomenclature suggests.

EBFs successfully combine the high level of ductility of MRFs and the high level of stiffness of CBFs by introducing eccentricity, e , between a frames cross bracing and column (Popov & Engelhardt, 1988). The cross brace of an EBF provides the elastic stiffness of CBF and the eccentricity of the cross brace creates a link that is responsible for the ductility and, therefore, energy dissipation capacity of MRF. The following sections describe the behavior of the link of an EBF; all other frame components are intended to remain elastic, and as such, adhere to conventional elastic behaviors.

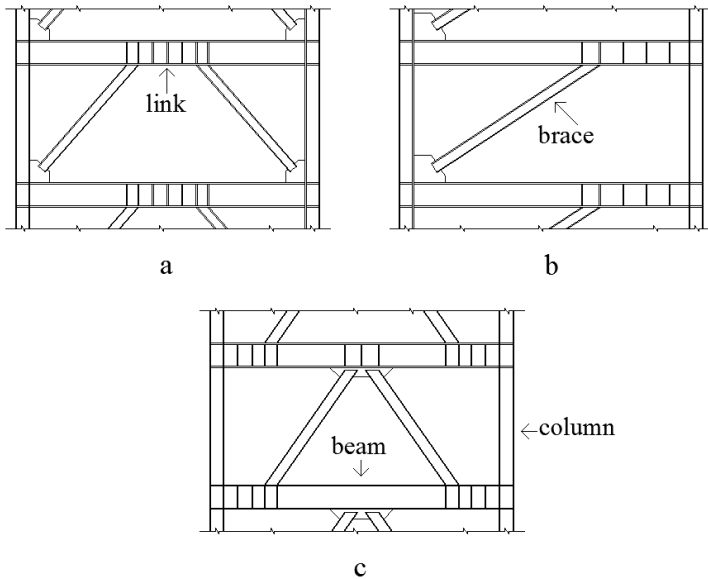


Figure 3-1: Eccentric Brace Frame Configurations

Link Length and Behavior

The link of an EBF experiences three forces: shear, axial, and flexural. Axial forces have been shown to be negligible for cases where link required axial strength, P_u , is marginal compared to nominal axial yield strength, P_y (Kasai & Popov, 1986). Discussion of the effects of axial loading continues in the following sections. Depending on the length of the link, either shear or flexural forces will dominate failure behavior. The standard nomenclature for links where behavior is dominated by shear and flexure is shear links and flexure links, respectively. In addition, due to inelastic behavior, a third classification arises that is dominated by a combination of shear and flexural yielding; links of such length are called intermediate links. The following sections describe the behavior of link elements based on the length ratio, ρ_o :

$$\rho_o = e / M_p / V_p \quad (\text{Equation 3-1})$$

where

ρ_o = length ratio

e = link length

$M_p =$ plastic moment

$V_p =$ plastic shear

Prior to the 1990s, research concerning EBFs primarily focused on shear links. Regardless, a number of LFRS incorporated EBFs with ρ_o -values larger than the shear link limit (Engelhardt & Popov, 1992). Longer link lengths allow for greater architectural and functional freedom within the LFRS; however, the usage of large ρ_o -values decreased the level of certainty at which engineers could ensure that failure would occur in the prescribed ductile manner. As a result, research into the behavior and effectiveness of longer links began to appear. At present, long-link behavior is better understood, allowing for greater architectural and functional freedom with a high level of certainty.

A Theoretical Link

The theoretical limit between behavior dominated by shear and flexure is based on simple plastic theory. For a link in equilibrium, shown in Figure 3-2, shear and flexural yielding occur simultaneously. From statics, the length ratio for theoretical balanced failure is 2.0.

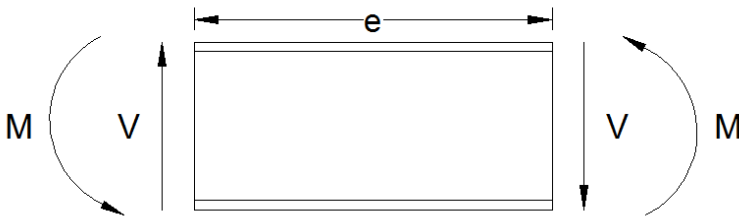


Figure 3-2: Static Equilibrium of Link Element

For $\rho_o < 2.0$, the link will reach full plastic shear capacity before full plastic moment capacity and, therefore, yield in shear, and vice versa. However, links do not behave as plastic theory suggests; links experience marginal interaction between shear and moment with or without axial loading, but strain hardening has significant effects (Kasai & Popov, 1986). For that reason, there is a range of length ratios in which failure behavior transitions from shear yielding to flexural yielding for increasing length ratios.

Strain Hardening

Within an EBF, the link element is designed to undergo severe inelastic deformation. During an extreme seismic event, the link may experience strain on a magnitude that induce strain hardening. Figure 3-3 illustrates an idealized stress-strain curve for structural steel; for strain hardening to occur, the structure must pass through two stages of behavior.

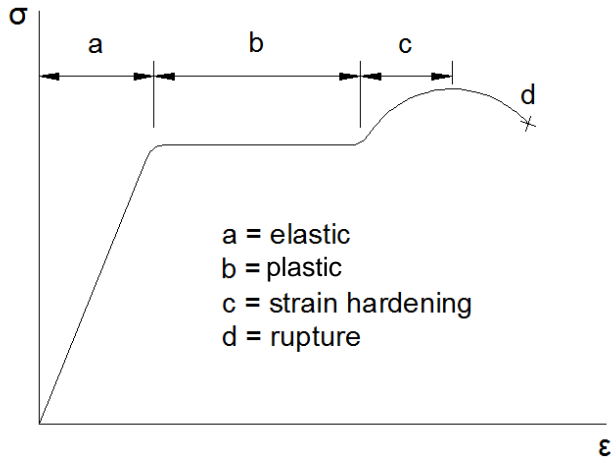


Figure 3-3: Idealized Structural Steel Stress-Strain Curve

During low loading, a structure should remain in region “a,” the elastic range; in the elastic range an increase in stress results in a linear increase in strain related to the modulus of elasticity, E of the structural material. During moderate loading, a structure may enter region “b,” with the transition between “a” and “b” characterized by inelastic (non-linear) behavior. In region “b,” the strain increases at a constant stress level, or behaves plastically. During plastic deformation, permanent residual deformations occur though the deformations may not be detrimental to the structural capacity upon unloading. After the structure’s plastic capacity is reached, additional inelastic behavior occurs as strain hardening; during strain hardening, the structure can undergo further deformation with a non-linear increase in stress. After the maximum tensile load is reached, necking occurs in members as strain continues to increase. During necking, the cross-sectional area of the seismic fuse in the LFRS decreases reducing the stress; as strain continues to increase the member ruptures, indicated by point “d” in Figure 3-3.

Recent research has shown that the magnitude of overstrength, or additional capacity after yield, for ASTM A992 steel is 1.3 on average; AISC 341 has adopted a link overstrength factor of 1.25. Any additional material overstrength is accounted for in R_y , the ratio of expected yield stress to the specified minimum yield stress (Arce, Okazaki, & Engelhardt, 2001).

Shear Links

Strain hardening in the link element requires the reduction of the shear link length ratio limit from 2. Furthermore, as a link element experiences large rotation angles, large end moments and steep strain gradients develop causing large flange strain. Large flange strain leads to instability in the form of web buckling after yielding; for unstiffened webs, web buckling occurs very shortly after shear yielding. Web buckling of shear links causes a severe reduction in load-carrying capacity, reducing energy dissipation and ductility (Kasai & Popov, 1986). Equally spaced web stiffeners preclude web buckling, which allows end moments to increase beyond M_p resulting in larger flange strain. To prevent flange weld failure, the maximum permissible moment for desirable shear link behavior is $1.2M_p$. The corresponding shear for the bounded moment is approximately $1.5V_p$. When M and V of Figure 3-2 correspond to $1.2M_p$ and $1.5V_p$, from statics the maximum ρ_o for shear links becomes 1.6 (Popov & Engelhardt, 1988).

Intermediate Links

The lower bound for intermediate link elements is a length ratio of 1.6. As ρ_o approaches the theoretical boundary, link failure involves shear and flexural yielding. Assuming the link moment is equally distributed between the link ends, link behavior will occur in a progression similar to the following:

1. Flexural yielding of the link flanges at both ends
2. Flexural yielding of the top flange of the brace panel
3. Shear yielding of the link web
4. Local buckling of the link flanges

After local buckling of the link flanges, which can be severe in appearance but not strength reduction, link behavior depends on the slenderness of the flanges. For the following discussion, the term slender flange does not necessarily indicate the flange does not meet AISC 341 or AISC 360 slenderness limits; rather, the flange is slender relative to more stocky flanges. As link elements are the seismic fuse of EBFs, they must display highly ductile behavior; as such, slenderness limits must preclude local failures that cause rapid strength degradation. Research has shown that for links with slender flanges, severe flange buckling of the top flange of the brace panel directly outside the link succeeds shear yielding of the web and causes rapid degradation of load-carrying capacity upon continued cyclic loading (Engelhardt & Popov, 1992).

For flanges that meet or exceed the slenderness limit of AISC 341, link flange local buckling is mild compared to that of slender flanges. Mid-frame links designed in accordance with AISC 341 will likely not experience further instability precluding failure; however, links connected to column faces typically experience fracture of the link flange at the link-to-column connection. For that reason, no prequalified connections for link-to-column connections exist (Okazaki, Engelhardt, Nakashima, & Suita, 2006).

The length ratio range for intermediate links of AISC 314 is $1.6 < \rho_o < 2.6$. However, the upper limit of 2.6 may not accurately reflect behavior of links. Experimental data from multiple test programs have shown that transitional behavior is strongly prevalent in links with $\rho_o \cong 2.6$. From the data, it has been recommended that the upper limit be increased to 3.0; however, AISC 341 reflects the limits first recommended in the 1988 model EBF code of the Structural Engineers Association of California (Engelhardt & Popov, 1992).

Flexure Links

Links with $\rho_o > 2.6$ are designated flexural links by AISC 341, though, as discussed in the previous section, combined behavior may still occur in links with ρ_o -values near the lower boundary. As ρ_o increases above 3.0, flexural yielding dominates inelastic behavior. The progression of yielding and instability is similar to that of intermediate links without web yielding and instability only occurring near the ends of a link. Yielding and instability for flexural links occurs in the following order, assuming equally distributed link end-moments:

1. Flexural yielding of link flanges at both ends
2. Flexural yielding of the top flange of the brace panel
3. Flexural yielding of previously yielded flanges increases in severity

Following the increased flexural yielding, link behavior depends on the slenderness of the flanges, as with intermediate links. For the following discussion, the term slender flange does not necessarily indicate the flange does not meet AISC 341 or AISC 360 slenderness limits; rather, the flange is slender relative to more stocky flanges. For slender flanges, the first form of link stability is flange buckling at the link ends; the flange buckling is typically not detrimental to link capacity. Following link flange buckling, brace panel top-flange buckling typically occurs that increasingly reduces load-carrying capacity with successive load cycles. For stocky flanges, very mild flange buckling may develop at both link ends with no other instability inside or outside of the link. As the length ratio becomes increasingly large ($\rho_o \approx 4$), flange instability is precluded by lateral torsional buckling in both the link and beam element. Lateral torsional buckling causes the load-carrying capacity significantly decreases; in addition, the out-of-plane movement induces out-of-plane forces in the link end lateral supports (Engelhardt & Popov, 1992).

Per AISC 341, there is no direct upper bound for ρ_o , but overall behavior of the structure must be taken into consideration. Rather, as link length increases, frame behavior more closely resembles that of a moment frame. Increased frame flexibility causes increased story drift, which serves as an indirect upper bound for link length for strength-controlled frames (Hjelmstad & Popov, 1984).

Link Rotation and Stiffness

Link rotation is the primary method of energy dissipation for EBF. In particular, as a link yields in shear or flexure, plastic hinges form allowing link rotation and frame deformation. For that reason, link webs must be adequately stiff to prevent premature web buckling that leads to sudden loss in load-carrying capacity and plastic rotation capacity (Popov & Engelhardt, 1988). For links with $\rho_o < 1.6$, after web yielding the dominating local instability is web inelastic buckling. A factor of great importance to web inelastic buckling is the ratio of the minimum unstiffened link panel dimension to the thickness of the web plate. Therefore, decreasing the

unstiffened link panel dimension or thickening the web will forestall the inelastic web buckling. However, the addition of welded doubler plates is not permitted as the desired composite action is seldom reached (Hjelmstad & Popov, 1983). As such links must be properly stiffened to allow for adequate rotation without web buckling.

To determine the link rotation angle, the EBF is assumed to deform in a rigid-plastic mechanism. Link rotation demand grows rapidly as link length decreases, as shown in Figure 3-4. The upper and lower bounds of 1.0 and 0 for e/L represent MRFs and CBFs, respectively. The large rotational demand can be met by links that yield in shear; however, as links become too short ($e/L \approx 0.10$), the inelastic strain required to achieve the rotational demand can result in brittle failure (Popov & Engelhardt, 1988).

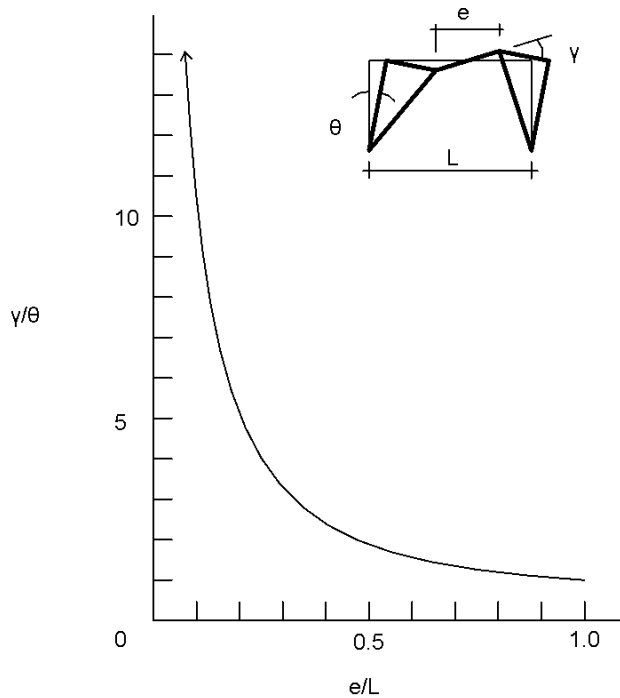


Figure 3-4: Link Rotation Demand

The rotation demand for EBFs in the link-to-column configuration is significantly lower. For shear links, this configuration is advantageous when the link rotation capacity is the limiting design factor; however, for longer links, link-to-column configurations have not been successfully configured to provide stable inelastic behavior up to prescribed inelastic rotations (Popov & Engelhardt, 1988); further discussion of link-to-column connection behavior follows.

Link Connections

This section primarily discusses the behavior of link elements in link-to-column connections. For mid-beam links, the link-brace connection must be able to resist the amplified seismic forces from the link in combination with the other loads from the governing load combination. This is easily accomplished with a CJP weld at the brace flanges. Link-brace connections are not discussed further, as in mid-beam link and link-to-column connections, there have been no issues during finite element analyses or lab test specimens at the beam end of the link.

In link-to-column connections, however, the moment at the column is generally larger than at the beam. The column connection attracts greater moment because the axial stiffness of the column is stiffer than the flexural stiffness of the beam; therefore, the true moment distribution for a link placed next to a column is similar to that of Figure 3-5. Upon first yield, which would occur near the column face, typical indeterminate structures experience moment redistribution. Moment redistribution is the redistribution of moment above the plastic capacity of the first yield section to sections of the member that are still elastic.

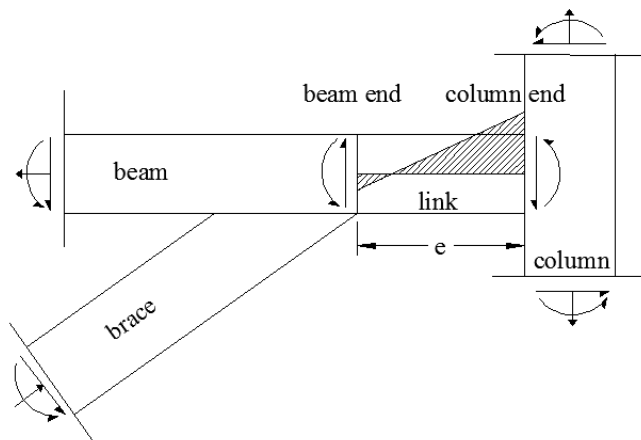


Figure 3-5: Link-to-Column Moment Distribution

In EBF link-to-column connections, traditional moment redistribution does not occur (Hjelmstad & Popov, 1983). Following the loading protocol in the 2005 *AISC Seismic Provisions* that decreased the link rotation angle at a given cycle number from the 2002 *AISC*

Seismic Provisions, similar to the methodology used for MRFs, link-to-column performance was expected to improve. Comparing results from each loading protocol, the link rotation capacity did increase remarkably; however, shear links continue to exhibit the non-ductile failure of fracture of the link web at the stiffener weld (Okazaki, Arce, Ryu, & Engelhardt, 2005). Further examination of four new link-to-column connection configurations yielded similar findings in that the majority of test specimens, which included shear, intermediate, and flexural links, experienced link web fracture at the stiffener weld. Link web fracture dominates testing as the link stiffeners provide such a large amount of buckling control (Okazaki, Engelhardt, Nakashima, & Suita, 2006). This research was undertaken to develop a prequalified link-to-column connection; the results reflect the current lack of a prequalified connection, though the 2010 *AISC Seismic Provisions* have exceptions to conformance demonstrations of proposed connections to provide designers with some latitude.

Chapter 4 - Design of Eccentric Brace Frame

In this chapter, the design requirements for an EBF according to AISC 341-10 are presented. The loads applied to the building and frames are found using Load and Resistance Factored Design (LRFD) methodologies within ASCE 7-10.

To determine member forces within the EBFs, the minimum design loads calculated from the ASCE 7 are distributed throughout the structure. Member forces are combined using LRFD load combinations from ASCE 7 Sections 2.3 and 2.4 with seismic modifications in Sections 12.4.2.3 and 12.4.3.2.

In an EBF, energy dissipation through yielding is intended to occur primarily in the link. Consequently, the beam and brace of the EBF must have the elastic capacity to resist the full inelastic-yielded, strain-hardened capacity of the links. The following sections outline the design requirements of an EBF's elements.

Link Design

The link of an EBF is greatly impacted by its length. The inelastic response of links with length shorter than $1.6 M_p/V_p$, where M_p and V_p are the plastic moment and shear capacity of the link, respectively, is governed by shear yielding. For links with length greater than $2.6 M_p/V_p$, the inelastic response is governed by flexural yielding. Intermediate link lengths will experience an inelastic response of combined shear and flexural yielding. The majority of the experimental analyses of EBFs were performed with shear links; furthermore, shear links generally have the greatest capacity for inelastic deformation. For these reasons, shear links are the recommended link type for EBFs (Building Seismic Safety Council, 2004), though intermediate and flexural links can successfully be implemented.

Shear Strength

Link shear strength is outlined in Section F3-5.b.(2) of AISC 341. The nominal shear strength is the lesser of the shear value obtained from analysis of shear yielding in the web and flexural yielding of the gross section. For shear yielding, the nominal shear strength is the plastic shear strength, V_p , depending on the ratio of ultimate axial force to axial force at yield:

$$V_p = 0.6F_y A_{lw} \text{ for } P_u/P_y \leq 0.15 \quad (\text{Equation 4-1})$$

$$V_p = 0.6F_y A_{lw} \sqrt{1 - (P_u/P_y)^2} \text{ for } P_u/P_y > 0.15 \quad (\text{Equation 4-2})$$

where

F_y = specified minimum yield stress

A_{lw} = link web area

P_u = required axial strength

P_y = nominal axial yield strength

For flexural yielding, the nominal shear strength is determined through the static relationship with M_p and e , rather:

$$V_n = 2M_p/e \quad (\text{Equation 4-3})$$

where

$$M_p = F_y Z \text{ for } P_u/P_y \leq 0.15 \quad (\text{Equation 4-4})$$

$$M_p = F_y Z \left(\frac{1 - P_u/P_y}{0.85} \right) \text{ for } P_u/P_y > 0.15 \quad (\text{Equation 4-5})$$

As discussed previously, the effect of marginal axial loading can be neglected in determining link strength. As the ratio of required axial strength to nominal yield strength increases above 15%, the plastic interaction between shear and moment is affected. To account for the reduction in strength caused by axial loading, a reduction factor is applied to the plastic moment capacity.

Link Length

For links with $P_u/P_y \leq 0.15$, when the effects of axial loading can be neglected, there is no upper limit on link length. Flexural links with low axial load exhibit reliable inelastic behavior (Engelhardt & Popov, 2003); however, the effect of moderate to large axial load on links that experience flexural yielding has not been extensively studied, so for links with $P_u/P_y > 0.15$ equations F3-10 and F3-11 of AISC 341 limit the link length based on the ratio of utilized axial strength to utilized shear strength, below.

$$e \leq 1.6M_p/V_p \text{ when } \rho' \leq 0.5 \quad \text{Equation 4-6}$$

$$e \leq \frac{1.6M_p}{V_p} (1.15 - 0.3\rho') \text{ when } \rho' > 0.5 \quad \text{Equation 4-7}$$

where

$$\rho' = (P_u/P_y)/(V_u/V_y)$$

Rotation Angle

In EBFs, the inelastic demand should not exceed the inelastic capacity of the links. As the inelastic capacity of an EBF is indicated by the link rotation angle, the link rotation angle is limited based on ρ_o . For links with $\rho_o \leq 1.6$, the plastic link rotation angle, γ_p , shall not exceed 0.08 rad. For links with $\rho_o \geq 2.6$, γ_p shall not exceed 0.02 rad. Intermediate link rotation angle limits are linearly interpolated between the limit for shear and flexural links. Estimates of the link rotation angle are possible by assuming the EBF will deform in rigid, plastic manner, as shown in Figure 4-1.

From Figure 4-1, the link rotation angle can be estimated through its geometric relationship with the plastic story drift angle, θ_p , as follows:

$$\gamma_p = \frac{L}{e} \theta_p \quad \text{(Equation 4-8)}$$

where

γ_p = plastic link rotation angle

θ_p = plastic story drift angle

L = frame length

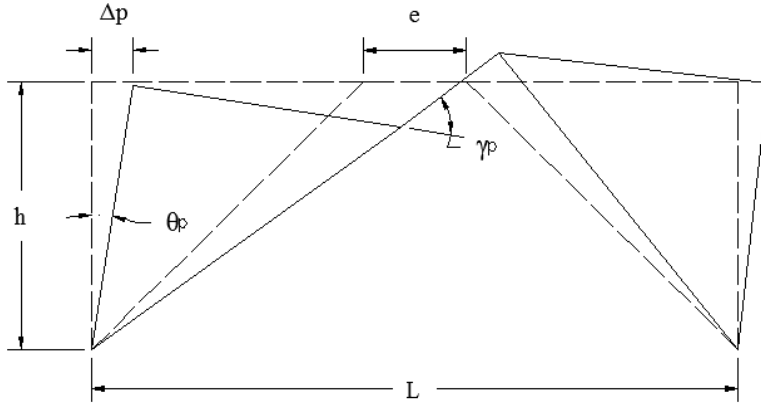


Figure 4-1: Link Rotation Angle

As θ_p is marginal, small deformation theory applies and the trigonometric function can be eliminated resulting in the following relationship:

$$\theta_p = \Delta_p/h \quad \text{(Equation 4-9)}$$

where

Δ_p = plastic story drift

h = frame height

In turn, the plastic story drift can conservatively be taken as the difference between the inelastic design story drift and the elastic design story drift, as only inelastic rotation is limited to the previous values. For greater accuracy, inelastic dynamic analysis is required.

Stiffeners

Full depth web stiffeners are required on both sides of the link web at the brace interfaces on all links. Web stiffeners must be fillet welded to the link web and flanges and be detailed to avoid welding in the k-region of the link, as reduction in the plastic rotation capacity of the link can occur when welds extend into the k-region (Okazaki, Engelhardt, Nakashima, & Suita, 2006). These stiffeners transfer link shear forces to the connected members and prevent web buckling. Per AISC 341, each side of each end shall have a stiffener at least $(b_f - 2t_w)/2$ and a thickness of at least the greater of $0.75t_w$ or 3/8 inch, with dimensions referring to the link

flange and web. To preclude premature failure of link elements due to excessive yield or instability, intermediate stiffeners are required based on the link type. Link stiffener requirements for shear links are based on research by Kasai and Popov (1986); for flexure links, requirements are based on research by Engelhardt and Popov (1992). Shear and flexure links each have independent stiffener requirements as they have different limit states, while intermediate links must meet the requirements of both shear and flexure link stiffeners. Intermediate web stiffeners must be full depth, and for links with a depth greater than 25 inches, intermediate web stiffeners are required on both sides.

Links with $\rho \leq 1.6$ experience shear yielding, so intermediate web stiffeners must be provided along the full length of the link. The maximum spacing depends linearly on γ_p . For $\gamma_p = 0.08$, the maximum spacing is $(30t_w - d/5)$. For $\gamma_p \leq 0.02$, the maximum spacing is $(52t_w - d/5)$. For γ_p between 0.08 and 0.02, the maximum spacing is determined using linear interpolation.

For links with $2.6 \geq \rho \geq 5$, the limit state is flexural yielding, so intermediate web stiffeners are only required near the link ends. Rather, per AISC 341 intermediate web stiffeners are required at a distance $1.5b_f$ from each link end.

Bracing

To further guard against instability, such as lateral-torsional buckling, that could lead to severe loss of strength, links must be laterally braced at the top and bottom at each end. A composite deck may provide adequate top flange bracing, but composite action cannot be counted on to brace the bottom flange (Popov & Engelhardt, 1988). As the link is expected to experience forces beyond the plastic capacity, the bracing must comply with the requirements for bracing at expected plastic hinge locations per AISC 341 D2.2c. The following equations are the required strength and stiffness, respectively:

$$P_u = 0.06R_yF_yZ/h_o \quad \text{(Equation 4-10)}$$

where

P_u = required lateral brace strength

h_o = distance between flange centroids

$$\beta_{br} = \frac{1}{\Phi} \left(\frac{10M_u C_d}{L_b h_o} \right) \quad \text{Equation 4-11}$$

where

$$M_u = R_y F_y Z$$

C_d = coefficient relating relative brace stiffness and curvature

Within Equation 4-11, C_d is 1.0, as the braces experience single curvature, and $\Phi = 0.75$.

Beam Design

The design of the beam outside of the link is based on the amplified seismic load from the link. Per AISC 341, the adjusted shear strength of a link is the nominal shear strength multiplied by the ratio of the expected yield strength to the minimum specified yield strength and the overstrength factor, 1.25, due to strain hardening. AISC 341 permits the overstrength factor to be reduced by a factor of 0.88 for beams outside of the link, so the overstrength factor becomes 1.1. This reduction is permitted as composite floor slabs substantially increase beam strength (Ricles & Popov, 1989). Moreover, limited yielding of the beam has been shown not to be detrimental to performance as long as the beam remains stable. It should be noted that the actual forces in the beams are greater than the forces computed with the reduced overstrength factor, but limited yielding and the composite slab make up for the deficit in required strength. If floor slabs are not composite, the Provisions do not limit the use of the reduction factor, but without composite action, the stability of the beam may be compromised (AISC 341).

Complications in EBF beam design arise when the beam outside of the link is inadequate to resist the strength required based on the ultimate link forces. The beam and link segments are typically the same member, so increasing the beam size results in an increased ultimate link force that the beam must resist. In order to address this issue, using shear links instead of longer links will reduce the link ultimate forces; additionally, specifying a brace with large flexural stiffness can reduce the demand on the beam, as more of the link moment would be transferred to the brace. The brace-link connection would need to be designed to resist the additional moment as a fully restrained moment connection (AISC 341).

Per AISC 341, beams outside of the link must meet the requirements of moderately ductile members. As the beam outside of the link is typically the same member as the link element, beams typically exceed ductility requirements in satisfying the requirements of the highly ductile link.

Brace Design

Unlike other brace frame LFRSs, EBF brace members are designed to remain elastic during an extreme seismic event. As such, the design is based on the capacity of the link; rather, a brace must be designed to resist load combinations including the amplified seismic load to account for the fully yielded and strain-hardened capacity of the link. In the case of EBFs, the amplified seismic load is the 1.25 times the expected nominal shear strength of the link, $R_y V_n$ (AISC 341).

The inherent configuration of EBFs induces significant axial loads and bending moments into braces; as such, braces are designed as beam-columns. Braces are typically designed as fully restrained at the link connection and pinned at the column connection. This allows the transfer of moment between the link and brace, which reduces the flexural demand on the beam outside of the link, as discussed previously (AISC 341).

EBF configurations typically have the brace centerlines intersecting each end of the link. Another method to address the design issue of inadequate strength of the beam outside of the link permitted by AISC 341 is to introduce eccentricity between the brace centerline and link end. By moving the centerline of the brace within the link, as shown in Figure 4-2, a moment is generated in the opposite direction of the link end moment; logically, the eccentricity should not be located outside of the link element unless the beam has excess flexural capacity, as the induced moment will be additive to the link end moment. AISC 341 permits connection eccentricities equal to or less than the beam depth if the inelastic deformation capacity is unaffected and the eccentricity is accounted for in design.

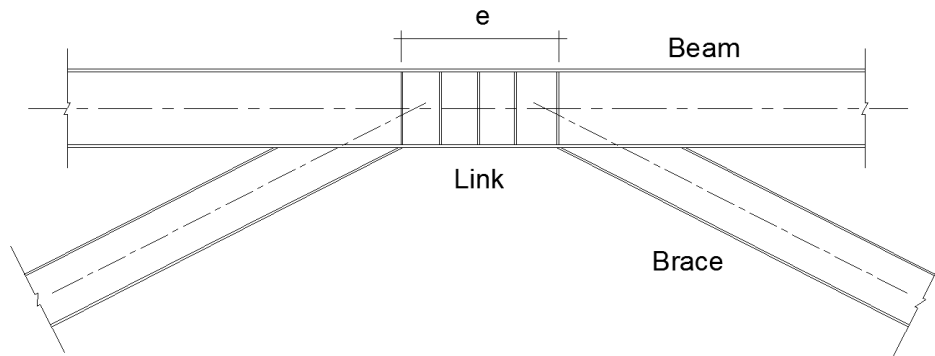


Figure 4-2: EBF with Interior Eccentric Brace

Per AISC 341, brace members must meet the requirements of moderately ductile members, as brace members should not experience any inelastic deformation.

Column Design

EBF column design requirements are similar to those of braces and beams outside of the link. As the link element is the only frame component designed to undergo inelastic deformation, columns are designed using capacity design principles; therefore, the amplified seismic load used in the seismic load combinations is determined using the force generated by a fully yielded and strain-hardened link. Therefore, columns must be designed to resist the combined fully yielded and strain-hardened forces from all links above the column.

Similar to beams outside of the link, in EBF columns the factor accounting for strain hardening in the amplified seismic load can be reduced by a factor of 0.88 in frames of three or more stories. This reduction is permissible, as the likelihood of all links above the column reaching their maximum shear strength simultaneously is low (Richards P. W., 2009). If all links do not reach their maximum shear strength simultaneously, designing for fully strain hardened links with a factor of 1.25 will be overly conservative; as a result, R_y can be reduced to 1.1. The 0.88 reduction factor is the quotient of the reduced R_y to the maximum expected R_y . For structures less than three stories, there is a greater likelihood that all of the links above the column will reach full strength simultaneously, so columns should be designed for the simultaneous, fully-strain-hardened links.

Connections

This section discusses the design requirements for connections in EBFs.

Demand Critical Welds

All welds in a SFRS must meet the specification of the Structural Welding Code-Seismic Supplement (AWS) Section D1.8. Demand critical welds are welds that could be exposed to yield-level strains during an extreme seismic event; therefore, demand critical weld requirements are more stringent. The locations within an EBF where demand critical welds are required by AISC 341 are as follows:

1. Groove welds at column splices
2. Welds at column-to-base plate connections
3. Welds at beam-to-column connections conforming to Section F3.6b(b)
4. Welds attaching the link flanges and the link web to the column where links connect to columns
5. Welds connecting the webs to the flanges in build-up beams within the link

At each of the listed locations, inelastic strain is expected. Further, the overall effect of brittle failure at some of these locations is not fully understood, so additional conservatism is needed, and is therefore included in the body of AISC 341 (AISC 341).

Beam-to-Column Connections

AISC 341 allows multiple design procedures for beam-to-column connections within EBFs. The connection may be designed in accordance with AISC 360 Section B3.6a as a simple connection; simple connections allow the beam to rotate relative to the column. EBFs have large rotations between beams and columns as story drifts near the service maximums are expected. If joints are not designed to accommodate the large rotation, especially a connection utilizing gusset plates, connections can be susceptible to rupture. For that reason, simple beam-to-column connections in EBFs must be able to withstand a rotation of 0.025 radians.

Beam-to-column connections may also be designed to resist the lesser moment from the following conditions:

1. The expected beam flexural strength, $R_y M_p$, multiplied by 1.1
2. The sum of expected column flexural strengths, $\sum R_y F_y Z$, multiplied by 1.1

Each condition must be examined with other connection and diaphragm forces. Each case must meet the same requirements as ordinary moment frames and will therefore provide a greater amount of system strength (AISC 341).

Brace Connections

As the brace is expected to remain elastic, both end connections must be able to withstand the required strength of the brace; that is, the most severe load case including the portion of the amplified seismic moment, shear, and axial load expected to be transferred to the brace. For braces that are designed to resist a portion of the link end moment, the brace connection at the link must be designed as fully restrained; the other brace connection is designed as a pinned connection.

Elastic and Inelastic Drift Considerations

After frame members have been sized, the frame story drift should be checked. Elastic joint displacements, δ_{xe} , are typically determined using structural analysis software in conjunction with load combinations 5, 6, and 7 of ASCE 7 Section 12.4.2.3. Using ASCE 7 Equation 12.8-15, the elastic joint displacements are used to determine the story drifts.

$$\delta_x = C_d \delta_{xe} / I_e \quad \text{(Equation 4-12)}$$

where

δ_x = amplified deflection at level x

C_d = deflection amplification factor

δ_{xe} = deflection at level x from elastic analysis

I_e = importance factor

The amplified story drifts are used to compute interstory drifts, which must be less than the allowable story drift to determine for the frame is adequate. The allowable interstory drift, Δ_a , is based on risk category and vertical LFRS type and is based on equations given in ASCE 7 Table 12.12-1.

For EBFs, link inelastic rotation is limited based on link length to control inelastic strain. Inelastic joint displacement can be estimated using the following static relationship:

$$\delta_{xie} = \delta_{xe}(C_d - 1)/I_e \quad \text{(Equation 4-13)}$$

where

$$\delta_{xie} = \text{inelastic deflection at level } x$$

Second-Order Analysis

AISC 360-10 Appendix 8 offers the approximate second-order analysis method, an alternative to a true second-order analysis, to account for second-order effects by amplifying first-order analysis required strengths. The approximate second-order method, hereafter referred second-order analysis, uses two factors to account for P- δ and P- Δ effects. P- δ effects result from members with combined axial and flexural loading that are out of plumb due to end moments. P- Δ effects result are a function of drift, which introduces eccentricity into the applied loads. Examples of each second-order effect are shown in Figure 4-3; the effects are magnified for illustrative purposes.

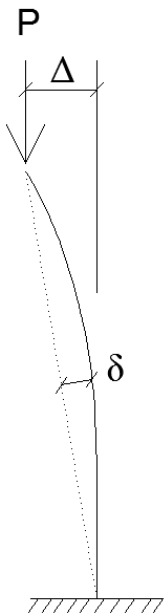


Figure 4-3: P-Delta Effects

Second-order required strengths are calculated using AISC 360-10 Equations A-8-1 and A-8-1, shown as Equation 4-14 and 4-15. Moments are amplified for P- δ and P- Δ effects while axial loads are only amplified for P- Δ effects.

$$\mathbf{M}_r = \mathbf{B}_1 \mathbf{M}_{nt} + \mathbf{B}_2 \mathbf{M}_{lt} \quad (\text{Equation 4-14})$$

$$\mathbf{P}_r = \mathbf{P}_{nt} + \mathbf{B}_2 \mathbf{P}_{lt} \quad (\text{Equation 4-15})$$

where

U_r = required second-order moment or axial strength

U_{nt} = first-order moment or axial force using load combinations with the structure restrained against lateral translation

U_{lt} = first-order moment or axial force using load combinations due to lateral translation of the structure only

B_1 = multiplier to account for P- δ effects (determined for each member)

B_2 = multiplier to account for P- Δ effects (determined for each story)

The following sections show the determination of the second-order analysis multipliers.

The B_1 Multiplier

P- δ effects are accounted for by the B_1 multiplier. B_1 is calculated using AISC 360-10 Equation A-8-3, as follows:

$$\mathbf{B}_1 = \mathbf{C}_m / (1 - \alpha \mathbf{P}_r / \mathbf{P}_{e1}) \geq 1 \quad (\text{Equation 4-16})$$

where

$C_m = 0.6 - 0.4 \left(\frac{M_1}{M_2} \right)$ for no transverse loading, or

$C_m = 1$ for transverse loading, conservatively

$\alpha = 1.6$ (ASD) or 1.0 (LRFD)

$P_r = P_u$ (first-order estimate is permitted)

P_{e1} = elastic critical buckling strength

$$P_e = \pi^2 EI / (K_e L)^2 \quad \text{(Equation 4-17)}$$

where

E = modulus of elasticity

I = moment of inertia in the plane of bending

K_e = effective length factor

L = length of member

The B_2 Multiplier

P - Δ effects are accounted for with the B_2 multiplier. B_2 is calculated using AISC 360-10 Equation A-8-6, as follows:

$$B_2 = \frac{1}{(1 - \alpha P_{story} / P_{e story})} \geq 1 \quad \text{(Equation 4-18)}$$

where

α = 1.6 (ASD) or 1.0 (LRFD)

P_{story} = total vertical load supported by the story

$P_{e story}$ = elastic critical buckling strength for the story

$$P_{e story} = R_M \left(\frac{HL}{\Delta_H} \right) \quad \text{(Equation 4-19)}$$

where

$R_M = 1 - 0.15(P_{mf} / P_{story})$

P_{mf} = total vertical load in the story that are part of moment frames (0 if braced frame)

L = story height

H = story shear

Δ_H = first-order interstory drift resulting from story shear, H

Chapter 5 - Parametric Study

This chapter discusses the parameters of the parametric study, an overview of the buildings within the study, the results of study, and general conclusions resulting from the study.

Parametric Study Overview

This report discusses and compares the design of EBFs. The comparison is based on the frame design for transverse lateral loading of on office building of two heights: two stories and five stories. The five-story building is further compared using two different second-order analysis assumptions: lateral displacement restrained and lateral displacement unrestrained; the second-order amplification factors for the two-story building are close to unity, so the results of a second-order comparison would be similar enough to disregard.

Each building height was chosen for specific purposes. The 2-story building was chosen to allow a simple comparison between the study in report by Eric Grusenmeyer (2012). The 5-story building was chosen after a process of elimination in an attempt to design the tallest efficient structure within the study parameters.

The building is located in Memphis, TN because of its moderately high seismic activity from the New Madrid fault system. Per ASCE 7-10, building height is not limited for a structure with an EBF LFRS in SDC “D.” The building plan, shown in Figure 5-1, is 120 feet (four bays of 30 feet) in the longitudinal direction and 75 feet (three bays of 25 feet) in the transverse direction. The stairs and elevators are assumed to be located outside the rectangular footprint to keep the floor plan symmetric and to not affect the design of the LFRS.

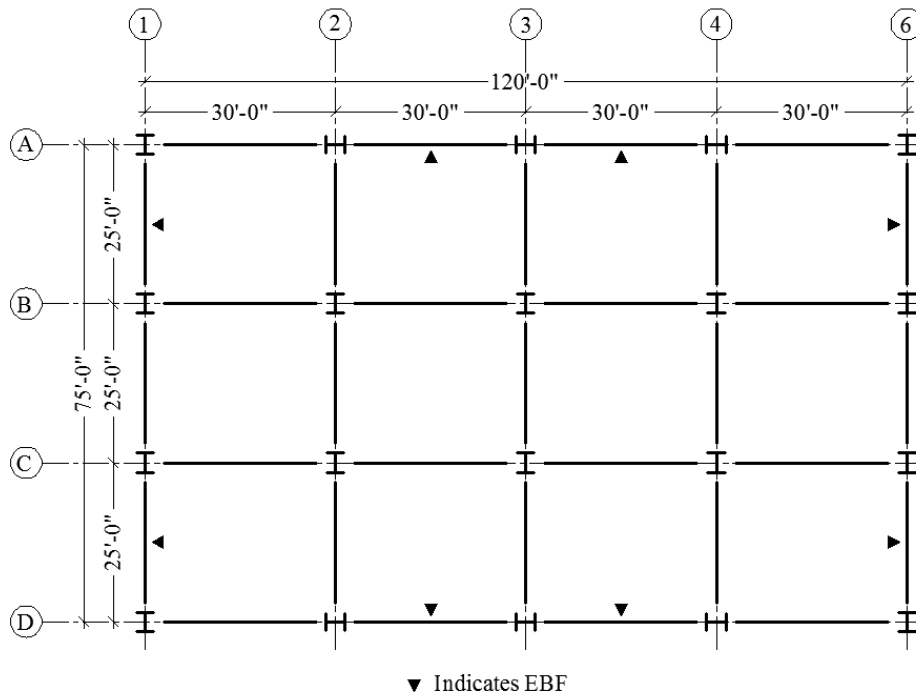


Figure 5-1: Building Framing Plan

The roof and floors are assumed to be rigid diaphragms of hollow core (HC) planks with lightweight concrete topping. The floor-to floor heights are 12 feet and the building has a parapet extending 2 feet above the roof level. Four brace frames are used in the transverse direction: two on each side of the building. Frame locations are indicated by ▼'s in Figure 5-1. The building envelope is a non-structural curtain wall system supported at each floor level. Figure 5-2 illustrates a transverse elevation of the five-story building.

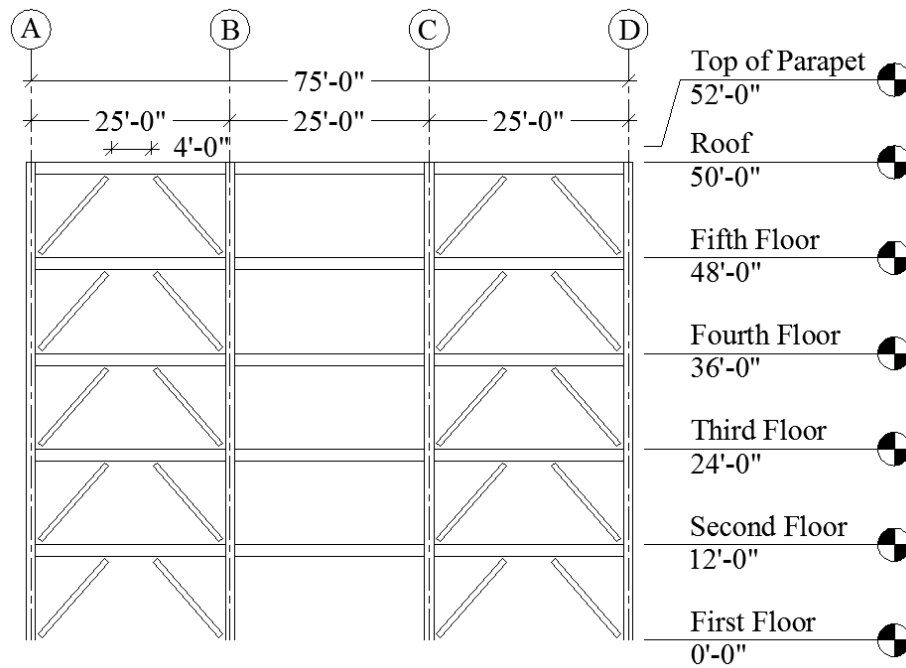


Figure 5-2: Five-Story Transverse Elevation

Seismic ground motion parameters were calculated using applicable equations and maps from ASCE 7-10. A geotechnical report was not used, as a specific location within Memphis, TN was not specified; for that reason, site class “D” was chosen based on ASCE 7-10 Section 11.4.2.

The computer analysis software RISA-3D was used to perform structural analysis of the buildings. Within RISA-3D, a two-dimensional frame consisting of one bay in which the EBF is located was modeled. Gravity loads were calculated and applied to the frame including loads from adjacent framing. Half of the seismic load for one side of the building was applied at each elevated level as point loads to each frame; rather one-quarter of the direct shear plus the resulting torsional shear per frame is applied to each frame. Per ASCE 7-10 Section 12.4.2.3, both seismic load combinations, shown on page 4 of this report, were considered. In this study, final member selection does not consider drift criteria due to gravity loading.

Governing Lateral Load

The lateral loads of this parametric study are as expected for high seismic regions with low to moderate wind pressures: in the transverse direction, seismic forces are approximately twice as large as wind forces for the two heights considered. This expectation should not, however, be applied to all buildings. For shorter buildings with larger plan dimensions, the seismic force is lower as the structural weight is typically less and closer to grade; furthermore, the wind force is typically higher due to the increased exposed surface area. Additionally, for buildings in the Brevard fault zone, which is near the border of North Carolina and South Carolina along the coast, buildings of moderate height and plan area could be governed by wind in one direction and seismic in another based on the type of LFRS and plan dimensions due to increased coastal wind pressures and high seismicity. In the event that wind forces govern over seismic forces, the LFRS must remain elastic up to the required wind forces, but still be detailed per seismic provision requirements to ensure ductile behavior in a seismic event.

Regardless of location, as the building height increases and approaches the flexible limit of 1 Hz, the equivalent seismic force increases at a lower rate. This is because the ELFP is a conservative linear, static estimate of the true non-linear, dynamic seismic event. As a building approaches the flexible limit, the ELFP introduces less conservatism. The wind and seismic base shears of all building heights investigated within this study are summarized in Table 5-1.

	Total Building Base Shear (kips)		Change in Base Shear (kips)	
	Wind	Seismic (R=8)	Δ Wind	Δ Seismic
2 Story	68	188	60	188
5 Story	190	393	122	205
7 Story	284	427	94	34
9 Story	385	455	101	28

Table 5-1: Base Shear Comparison

Results

The following section discusses the results of the parametric study, including member sizes and the percent stressed, interstory drift, and second-order amplification factors. The results of a study performed by Grusenmeyer (2012) on Special Concentrically Braced Frames are also discussed.

Member Sizes

Link members should ideally be limited to sections with nominal shear capacities near that of the required ultimate forces. This limitation is primarily because the link and beams outside of the link are typically a continuous section, and the beam must be able to resist the amplified seismic forces from the link. The overstrength factor used to determine the amplified seismic force is the ratio of the available shear capacity to the shear induced by ASCE-7 seismic forces; for that reason, as the link nominal shear capacity increases from the required capacity, the overstrength factor used to determine the amplified seismic forces also increases.

Preliminary link sections can be determined by finding link shear force induced by the vertically distributed seismic forces and the frame configuration through statics. The link shear is then used to find the minimum required shear area by rearranging the applicable equation for shear capacity per AISC 360.

Brace sections are geometrically limited by the link element. As the brace is designed to transfer a portion of the link end moment, reducing the demand on the beams, the brace-link connection must be designed as fully restrained. To accommodate this requirement, the width of the brace flange must be equal to or less than the width of the link flange to allow for full development of the CJP welds. As such, when B_2 was considered in second-order analysis of this study heavier brace sections within the same family as the link are only option to account for required strength and drift control.

Column elements are a vital means of drift control in EBFs, as they are not limited by the link element like braces. When B_2 second-order effects were considered, amplification of the translational moments and axial forces resulted in overstressed members within permitted drifts when the members from the translation-permitted study were used as a starting point. As such, the frames required an increase in lateral stiffness to reduced drift to meet combined loading requirements. As a result, the difference in column sizes between $P-\Delta$ considered and $P-\Delta$ not considered is the greatest among the member types. For the purpose of this study, columns are continuous in two story increments. Practically, column depth would not change between members to accommodate column splices; this requirement was not considered to illustrate the collection of forces at lower levels.

A comparison of member sizes for each second-order analysis condition for the 2-story and 5-story frame along with the percent stressed due to combined axial and flexural loading

considering second-order effects is shown in Table 5-2 and Table 5-3, respectively. Within Table 5-2 and Table 5-3, combined axial and flexural percent stressed values are presented at elastic levels, E, for links, and amplified seismic levels, AS, for beam and brace members. Links also have shear percent stressed, V, which is the ratio of the elastic seismic force to the available amplified seismic shear strength. For columns, the percent stressed is for amplified axial load, A, only, as the columns do not resist external moments.

2 Story	B ₂ - Approx. Unity	
Member	Section	Percent Stressed
Link		
Roof	W12x96	.115 _E / .073 _V
2nd	W12x96	.149 _E / .105 _V
Beam		
Roof	W12x96	.975 _{AS}
2nd	W12x96	.902 _{AS}
Brace		
2nd	W10x88	.896 _{AS}
1st	W10x100	.874 _{AS}
Column		
2nd	W12x96	.252 _A
1st	W12x96	.565 _A

Table 5-2: 2-Story Member Results

5 Story	B ₂ - Unity		B ₂ - Considered	
Member	Section	Percent Stressed	Section	Percent Stressed
Link				
Roof	W10x88	.148 _E / .091 _V	W10x88	.164 _E / .090 _V
5th	W10x88	.224 _E / .155 _V	W10x112	.218 _E / .123 _V
4th	W10x100	.237 _E / .181 _V	W12x120	.241 _E / .141 _V
3rd	W12x96	.244 _E / .211 _V	W12x136	.248 _E / .146 _V
2nd	W12x106	.233 _E / .2 _V	W12x136	.26 _E / .155 _V
Beam				
Roof	W10x88	.736 _{AS}	W10x88	.998 _{AS}
5th	W10x88	.793 _{AS}	W10x112	.99 _{AS}
4th	W10x100	.797 _{AS}	W12x120	.983 _{AS}
3rd	W12x96	.751 _{AS}	W12x136	.939 _{AS}
2nd	W12x106	.756 _{AS}	W12x136	.986 _{AS}
Brace				
5th	W10x68	.908 _{AS}	W10x112	.720 _{AS}
4th	W10x68	.95 _{AS}	W10x112	.889 _{AS}
3rd	W10x68	.925 _{AS}	W10x112	.866 _{AS}
2nd	W10x77	.835 _{AS}	W10x120	.912 _{AS}
1st	W10x88	.846 _{AS}	W12x136	.861 _{AS}
Column				
5th	W10x88	.179 _A	W18x97	.188 _A
4th	W10x88	.358 _A	W18x106	.388 _A
3rd	W10x100	.642 _A	W18x106	.635 _A
2nd	W12x120	.743 _A	W18x119	.790 _A
1st	W12x136	.85 _A	W18x119	.984 _A

Table 5-3: 5-Story Member Results

Story Drift

For the parametric study, the building story drifts were well within the ASCE 7-10 limits for EBFs. Table 5-4 shows the actual interstory drift by level for each frame considered. Table 5-5 then compares the average interstory drifts for each building height and second-order

consideration to the allowable interstory drift. The design drifts for when lateral translation is not considered are greater than when translation is considered. This is a result of the amplified lateral moments due to drift requiring a more efficient sections, which tend also to have larger moments of inertia.

Level	Interstory Drift (in)		
	2 Story	5 Story	
		No B ₂	B ₂
Roof	0.11	0.49	0.392
5th	-	0.54	0.412
4th	-	0.52	0.352
3rd	-	0.39	0.264
2nd	0.12	0.23	0.144

Table 5-4: Interstory Drift by Level

Frame	Interstory Drift Summary (in)		
	Allowable	B ₂ - Unity	B ₂ - Considered
		Design Average	Design Average
2-Story	3.60	-	0.115
5-Story	3.60	0.43	0.31

Table 5-5: Interstory Drift Summary

Second-Order Effects

One of the aims of this study was to examine how P-Δ effects affect the design of LFRSs. As such, for each building height, the frames of the LFRS were designed under two assumptions: lateral translation is restrained and lateral translation is unrestrained. Lateral restraint affects the B₂ multiplier in second-order analysis, which amplifies the factored moments and axial forces due to lateral translation of the structure. Table 5-6 shows the B₂ second-order amplification factor for the 2- and 5-story buildings. For the 2-story building, the first level has a 6% amplification. The 5-story building, however, has a 33% amplification due to the increase in column load and story shear. For the 5-story building, the value in parenthesis is the B₂ factor that results from member selection in the design not considering B₂ second-order effects to illustrate their magnitude even though they are not applied.

Story	B ₂ Factor	Story	B ₂ Factor
Roof	1.06	Roof	1.07 (1.23)
-	-	5th	1.16 (1.62)
-	-	4th	1.23 (2.03)
-	-	3rd	1.27 (2.21)
2nd	1.15	2nd	1.33 (2.43)

Table 5-6: Second Order Factors for 2- and 5-story Frames

Second-order effects are best illustrated in the design of tall buildings, as the increased moment arm between distributed lateral loads cause large deflections. In investigating the height limit for practical design within the conditions of the study considering second-order effects, buildings of nine and seven stories were eliminated due to the impracticality of second-order B₂ amplification. After optimization of the seven-story frame, the B₂ multiplier was approximately four at the first story. This value was obtained only after selecting heavy column sections, such as W33x263 and larger, to reduce significantly drift at lower floors. For frames taller than seven stories, however, the gains from increasing column stiffness would become less, as the B₂ multiplier is also a factor of the total vertical load supported by the columns of a level. With increasing frame height, the columns in the lower floors support increasing load, so even miniscule interstory deflection results in impractical second-order amplification within this study. This indicates that for structures similar in plan and loading to this study would require a dynamic analysis, which would inherently include second-order effects and allow for a design that is more efficient.

As mentioned previously, the columns are the primary means of drift control in EBFs, as the beam outside of the link and brace sections are limited by overstrength in the case of the beam and dimensional limits in the case of the brace. Increasing the link and beam size would increase the overall lateral stiffness of the frame; this would also allow for larger brace sections, which would also increase lateral stiffness. The beneficial effect of decreased drift, and B₂, due to increased lateral stiffness would be counteracted, as a column must be able to resist the total amplified shear strength of all links above the column.

Special Concentrically Braced Frames Comparison

This section compares the results of the two-story EBF frame from this study with the results of a study by Eric Grusenmeyer (2012) on a two-story Special Concentric Brace Frame. The building used in this and Grusenmeyer's study has the same plan and use, but the following variations must be noted:

1. The transverse LFRS has only one frame
2. The floor-to-floor height is 16'-0"
3. The roof and floor systems are metal deck with bar joists and composite metal deck with normal weight concrete topping, respectively
4. The building is located in Henderson, NV
5. The LRFS is assumed to be braced against lateral translation

For variation (3), the difference in roof and floor systems results in a significant difference in the effective seismic weight of the structure. This reduction is counteracted by the lower response modification coefficient of SCBFs in conjunction with variation (4), which results in different short- and long-term Design Spectral Response Acceleration Parameters. Per Grusenmeyer (2012), S_{DS} and S_{D1} for Henderson, NV are 0.542 and 0.253, respectively. For Memphis, TN, S_{DS} and S_{D1} are 0.691 and 0.374, respectively. These parameters along with the R , I_e , and T_a of each study result in a C_s of 0.0903 for Grusenmeyer's structure and 0.086 for this study's two-story structure. Combined with W 's 859.95 kips and 2179 kips, the seismic base shears per Grusenmeyer and this study are 77 kips and 188 kips, respectively.

The greater seismic base shear for the 2-story structure of this study warrants the use of two frames in the LFRS in the transverse direction. In Grusenmeyer's structure, the single frame must resist the full 77 kips that is vertically and horizontally distributed to and within each level. Within this study's 2-story structure, the each of the two frames is assumed to resist half of the distributed load. For that reason, variation (1) is accounted for as the lateral forces between the two studies are within enough reason to allow for a valid comparison.

The difference in results between Grusenmeyer's and this study as a result of variation (2) and (5) are minimal as the $P-\Delta$ B_2 magnification factor is less than 10% for this study's 2-story structure. It should be noted that SCBFs are a typically strength controlled due to the

stiffness of the bracing member reducing lateral translation. If B_2 was considered, the amplification would likely be on the same order of magnitude to that of this study due to the drift control provided by the concentric braces.

Table 5-7 outlines the final member selection of this study and compares them to Grusenmeyer's study of SCBFs in the chevron configuration. Within Table 5-7, combined axial and flexural percent stressed values are presented at elastic levels, E, for links, and amplified seismic levels, AS, for beam and brace members. Links also have percent stressed values for shear, V, which is the ratio of the elastic seismic force to the available amplified seismic shear strength. For columns, the percent stressed is for amplified axial load, A, as the columns do not resist external moments.

EBF			SCBF	
2 Story Member	B ₂ - Approx. Unity Section	Percent Stressed	2 Story Member	B ₂ - Unity Section
Link			-	
Roof	W12x96	.115 _E / .073 _V	No Link in SCBFs	
2nd	W12x96	.149 _E / .105 _V	-	
Beam			Beam	
Roof	W12x96	.975 _{AS}	Roof	W27x94
2nd	W12x96	.902 _{AS}	2nd	W30x124
Brace			Brace	
2nd	W10x88	.896 _{AS}	Roof	HSS4x0.22
1st	W10x100	.874 _{AS}	2nd	HSS5.5x0.258
Column			Column	
2nd	W12x96	.252 _A	2nd	W14x68
1st	W12x96	.565 _A	1st	W14x68

Table 5-7: Comparison of Two-Story EBF and SCBF (Grusenmeyer, 2012) Results

From Table 5-7, the beam sections of the SCBF are much larger than those of the EBF; the chevron configuration in a SCBF results in unbalanced beam loading due to one brace being in compression and one in tension. For that reason, the induced moment and axial force in the beam requires increased strength. In a SCBF, the inelastic behavior is limited to the braces; on the other hand, in an EBF, the inelastic behavior is limited to the links. As such, the brace of

SCBF is designed to resist the force induced by the distributed seismic load of the ELFP, while the brace of EBF is designed to resist a portion of the amplified link end moment and axial force. Therefore, the braces of SCBFs and EBFs must be compared considering their function. SCBF braces are the upper bound for stiffness of EBFs. As such, the braces of EBFs must have greater moments of inertia to provide similar stiffness; furthermore, EBF braces resist amplified seismic forces, so they must have greater plastic moduli and cross-sectional areas. In essence, SCBFs can have smaller braces, but in the chevron configuration must have larger beams.

Conclusions

Second-order effects in tall buildings are a major design consideration. Through the assumption that frames are braced against lateral translation, the lateral forces transmitted to the frame are not amplified to account for internal and end eccentricity. As illustrated in the 2-story frame of this study, structures 24 ft. and lower have minimal amplification; however, for structures above 24 ft. in height, P- Δ effects become significant and, therefore, cannot be neglected without under designing the structure.

The maximum reasonable height of a structure utilizing eccentrically braced frames is also related to second-order effects. As the number of stories in a structure increases, the column axial loads at lower levels increases. The B_2 multiplier related to P- Δ effects is linearly related to P_{story} . Additionally, the magnitude of vertically distributed seismic lateral forces increases as structural height increases; as a result, the without significantly increasing the flexural stiffness of frame members, interstory drift increases. The B_2 multiplier is also linearly related to interstory drift. To summarize, as building height increases, P_{story} increases, and ΔH has the potential to increase; as a result, the B_2 multiplier increases causing increasingly amplified frame forces. Through trials with 2-, 5-, 7-, and 9-story structures with the parameters of this study, all of which remained below the flexible limit of 1 Hz, second-order effects become impractical to design against for 7-story structures and taller (greater than 84 ft.). As a result, the structure would require dynamic analysis instead of the ELFP.

Brace axial force is limited by link buckling which precludes brace buckling; preclusion of brace buckling is advantageous as inelastic buckling results in hysteretic behavior that is less stable than that of yielding. For that reason, EBFs do not require special detailing of brace elements. Conversely, SCBFs rely on brace buckling as a means of energy dissipation. As such,

the brace connections must be designed and detailed to remain elastic during brace buckling or yielding. Furthermore, for the chevron configuration, the beams of a SCBF are required to resist the amplified seismic forces induced in the brace element resulting in increased beam sections. In EBFs, the amplified seismic force from the link element is shared by the brace and the beam outside of the link, resulting in economical beam and brace sections.

Overall, EBFs provide excellent seismic performance for extreme seismic loads for low-rise structures. As building height increase, the influence $P-\delta$ and $P-\Delta$ effects increase. Rather, the assumption that a structure is brace against lateral translation becomes increasingly invalid as building height increases.

References

- Building Seismic Safety Council. (2004). *NEHRP Recommended Provisions for Seismic Regulations for New Buildings and other Structures: FEMA 450 2003 Edition*. Washington, D.C.: Federal Emergency Management Agency.
- Arce, G., Okazaki, T., & Engelhardt, M. D. (2001). *Experiments on the Impact of Higher Strength Steel on Local Buckling and Overstrength of Links in EBFs*. Chicago: American Institute of Steel Construction.
- Engelhardt, M. D., & Popov, E. P. (1992). Experimental Performance of Long Links in Eccentrically Braced Frames. *Journal of Structural Engineering*, 118(11), 3067-3088.
- Engelhardt, M. D., & Popov, E. P. (2003). *Tests of Long Links in Seismic-Resistant Eccentrically Braced Frames*. Chicago: American Institute of Steel Construction.
- Grusenmeyer, E. (2012). *Design Comparison of Ordinary Concentric Brace Frames and Special Concentric Brace Frames for Seismic Lateral Force Resistance for Low Rise Buildings*. Master's report, Kansas State University, Manhattan, Kansas.
- Hjelmstad, K. D., & Popov, E. P. (1983). Cyclic Behavior and Design of Link Beams. *Journal of Structural Engineering*, 109(10), 2387-2403.
- Hjelmstad, K. D., & Popov, E. P. (1984). Characteristics of Eccentrically Braced Frames. *Journal of Structural Engineering*, 110(2), 340-353.
- Kasai, K., & Popov, E. P. (1986). General Behavior of WF Steel Shear Link Beams. *Journal of Structural Engineering*, 112(2), 362-382.
- Leyendecker, E. V., Hunt, R. J., Frankel, A. D., & Rukstales, K. S. (2000). Development of Maximum Considered Earthquake Ground Motion Maps. *Earthquake Spectra*, 16(1), 21-40.
- Minimum Design Loads for Buildings and Other Structures: ASCE 7-10*. (2010). Reston: American Society of Civil Engineers.
- Okazaki, T., Arce, G., Ryu, H., & Engelhardt, M. D. (2005). Experimental Study of Local Buckling, Overstrength, and Fracture of Links in Eccentrically Braced Frames. *Journal of Structural Engineering*, 131(10), 1526-1535.
- Okazaki, T., Engelhardt, M. D., Nakashima, M., & Suita, K. (2006). Experimental Performance of Link-to-Column Connections in Eccentrically Braced Frames. *Journal of Structural Engineering*, 132(8), 1201-1211.
- Popov, E. P., & Engelhardt, M. D. (1988). Seismic Eccentrically Braced Frames. *Journal of Constructional Steel Research*, 10, 321-354.

Richards, P. W. (2009). Seismic Column Demands in Ductile Braced Frames. *Journal of Structural Engineering*, 135(1), 33-41.

Seismic Provisions for Structural Steel Buildings: AISC 341-10. (2010). Chicago: American Institute of Steel Construction.

Bibliography

- American Institute of Steel Construction Manual* (14th ed.). (2010). Chicago: American Institute of Steel Construction.
- Arce, G., Okazaki, T., & Engelhardt, M. D. (2001). *Experiments on the Impact of Higher Strength Steel on Local Buckling and Overstrength of Links in EBFs*. Chicago: American Institute of Steel Construction.
- Berman, J. W., Okazaki, T., & Hauksdottir, H. O. (2010). Reduced Link Sections for Improving the Ductility of Eccentrically Braced Frame Link-to-Column Connections. *Journal of Structural Engineering*, 136(5), 543-553.
- Building Seismic Safety Council. (2004). *NEHRP Recommended Provisions for Seismic Regulations for New Buildings and other Structures: FEMA 450 2003 Edition*. Washington, D.C.: Federal Emergency Management Agency.
- Elnashai, A. S., & Mwafy, A. M. (2002). Overstrength and Force Reduction Factors of Multistory Reinforced-Concrete Buildings. *Structural Design of Tall Buildings*, 11, 329-351.
- Engelhardt, M. D., & Popov, E. P. (1992). Experimental Performance of Long Links in Eccentrically Braced Frames. *Journal of Structural Engineering*, 118(11), 3067-3088.
- Engelhardt, M. D., & Popov, E. P. (2003). *Tests of Long Links in Seismic-Resistant Eccentrically Braced Frames*. Chicago: American Institute of Steel Construction.
- Fuqua, B. W. (2009). *Buckling Restrained Braced Frames as a Seismic Force Resisting System*. Master's report, Kansas State University, Manhattan, Kansas.
- Grusenmeyer, E. (2012). *Design Comparison of Ordinary Concentric Brace Frames and Special Concentric Brace Frames for Seismic Lateral Force Resistance for Low Rise Buildings*. Master's report, Kansas State University, Manhattan, Kansas.
- Hashemi, S. H. (2011). Ductility and Ultimate Strength of Eccentric Braced Frame. *International Conference on Advanced Materials Engineering*, (pp. 68-74). Singapore.
- Hjelmstad, K. D., & Popov, E. P. (1983). Cyclic Behavior and Design of Link Beams. *Journal of Structural Engineering*, 109(10), 2387-2403.
- Hjelmstad, K. D., & Popov, E. P. (1984). Characteristics of Eccentrically Braced Frames. *Journal of Structural Engineering*, 110(2), 340-353.
- International Building Code*. (2012). Country Club Hills: International Code Council, Inc.
- Kasai, K., & Popov, E. P. (1986). General Behavior of WF Steel Shear Link Beams. *Journal of Structural Engineering*, 112(2), 362-382.

- Kasai, K., & Popov, E. P. (1986b). Cyclic Web Buckling Control for Shear Link Beams. *Journal of Structural Engineering*, 112(3), 505-523.
- Leyendecker, E. V., Hunt, R. J., Frankel, A. D., & Rukstales, K. S. (2000). Development of Maximum Considered Earthquake Ground Motion Maps. *Earthquake Spectra*, 16(1), 21-40.
- Mansour, N., Christopoulos, C., & Tremblay, R. (2011). Experimental Validation of Replacable Shear Links for Eccentrically Braced Steel Frames. *Journal of Structural Engineering*, 137(10), 1141-1152.
- Minimum Design Loads for Buildings and Other Structures: ASCE 7-10*. (2010). Reston: American Society of Civil Engineers.
- Moghaddam, H., & Hajirasouliha, I. (2008). Optimum Strength Distribution for Seismic Design of Tall Buildings. *Structural Design of Tall and Special Buildings*, 17, 331-349.
- Okazaki, T., Arce, G., Ryu, H., & Engelhardt, M. D. (2005). Experimental Study of Local Buckling, Overstrength, and Fracture of Links in Eccentrically Braced Frames. *Journal of Structural Engineering*, 131(10), 1526-1535.
- Okazaki, T., Engelhardt, M. D., Nakashima, M., & Suita, K. (2006). Experimental Performance of Link-to-Column Connections in Eccentrically Braced Frames. *Journal of Structural Engineering*, 132(8), 1201-1211.
- Popov, E. P., & Engelhardt, M. D. (1988). Seismic Eccentrically Braced Frames. *Journal of Constructional Steel Research*, 10, 321-354.
- Richards, P. W. (2009). Seismic Column Demands in Ductile Braced Frames. *Journal of Structural Engineering*, 135(1), 33-41.
- Richards, P. W., & Uang, C. (2005). Effect of flange Width-Thickness Ratio on Eccentrically Braced Frames Link Cyclic Rotation Capacity. *Journal of Structural Engineering*, 131(10), 1546-1552.
- Richards, P., Okazaki, T., Engelhardt, M. D., & Uang, C. (2007). Impact of Recent Research Findings on Eccentrically Braced Frame Design. *Engineering Journal*, 44(1), 41-53.
- Ricles, J. M., & Popov, E. P. (1989). Composite Action in Eccentrically Braced Frames. *Journal of Structural Engineering*, 115(8), 2046-2066.
- Seismic Provisions for Structural Steel Buildings: AISC 341-05*. (2005). Chicago: American Institute of Steel Construction.
- Seismic Provisions for Structural Steel Buildings: AISC 341-10*. (2010). Chicago: American Institute of Steel Construction.

Specification for Structural Steel Buildings: AISC 360-10. (2010). Chicago: American Institute of Steel Construction.

Whittaker, A., Hart, G., & Rojahn, C. (1999). Seismic Response Modification Factors. *Journal of Structural Engineering*, 125(4), 438-444.

Appendix A – Load Calculations

Live Load

ASCE 7-10 UNO

Roof Live Load =	20	psf	T. 4-1
Floor Live Load =	80	psf	T. 4-1
Corridor above 1st			

Dead Load

Roof Dead Load

1 Ceiling (Fiber Board + Channels)	3	psf	T. C3-1
2 Waterproof Bitum. w/ Gravel	5.5	psf	T. C3-1
3 Rigid Insul. (.75psf/.5in) 4"	6	psf	T. C3-1
4 3.5" LW Conc. Topping 8 psf/in	28	psf	PCIDesign
5 10" HC Planks	65	psf	Handbook
6 MEP	10	psf	T. C3-1
	<u>117.5</u>	psf	
	<u>120</u>	psf	

Floor Dead Load

1 Ceiling	3	psf	T. C3-1
2 3.5" LW Conc. Topping 8 psf/in	28	psf	PCIDesign
3 10" HC Planks	65	psf	Handbook
4 Flooring (Carpet)	1	psf	T. C3-1
5 MEP	10	psf	T. C3-1
	<u>107</u>	psf	
	<u>110</u>	psf	

Wall Dead Load

1 Glass Curtain Wall System	20	psf	T. C3-1
	<u>20</u>	psf	
	<u>20</u>	psf	

Flat Roof
Snow Load

$$p_f = 0.7C_eC_tI_sP_g$$

$$C_e = 1 \quad \text{Cat B Part. Exp.}$$

$$C_t = 1 \quad \text{T. 7-3}$$

$$I_s = 1 \quad \text{Risk Cat II} \quad \text{T. 1.5-2}$$

$$P_g = 10 \quad \text{psf} \quad \text{T. 7-1}$$

$$p_f = 7 \quad \text{psf}$$

Eqn 7.3-1

T. 7-2

T. 7-3

T. 1.5-2

T. 7-1

Minimum
Snow Load

$$P_m = I_sP_g$$

$$P_m = 10 \quad \text{psf}$$

Sec 7.3.4

Balanced
Snow Load
Height

$$h_b = p_f/\gamma$$

$$\gamma = 0.13P_g + 14 < 30$$

$$\gamma = 15.3 \quad \text{pcf}$$

$$h_b = 0.66 \quad \text{ft}$$

Sec 7.7.1

Eqn 7.7-1

Drift
Considerations

$$h_c/h_b = 2.03 > 0.2, \text{ consider drift}$$

$$\text{Parapet Height} = 2 \quad \text{ft}$$

$$h_c = 1.34 \quad \text{ft}$$

Windward Drift
(no leeward drift
condition)

$$h_d = 0.43(l_u)^{.333}(P_g+10)^{.25}-1.5 \quad \text{ft}$$

$$l_u = 120 \quad \text{ft}$$

$$h_d = 2.99 \quad \text{ft}$$

$$0.75h_d = 2.24 \quad \text{ft}$$

Fig. 7-9

$$w = 4h_d^2/h_c \quad 0.75h_d > h_c$$

$$w = 26.60 \quad \text{ft}$$

Sec 7.7.1

$$w_{max} = 8h_c$$

$$w_{max} = 10.72 \quad \text{ft}$$

Sec 7.7.1

$$h_d = h_c = 1.34 \quad \text{ft}$$

Sec. 7.7.1

$$p_d = \gamma h_d$$

$$p_d = 21 \quad \text{psf}$$

Sec 7.7.1

Basic Equation	$q = 0.00256K_zK_{zt}K_dV^2$	Eqn 27.3-1
and Wind	$K_{zt} = 1$ Flat Site	26.8.2
Pressures	$K_d = 0.85$ MWFRS	T. 26.6-1
	$V = 115$ MPH Cat. II	

Height	K_z (B)	q (psf)	
0-15	0.57	16.403	
20	0.62	17.842	
24	0.65	18.705	(Top of Structure)
25	0.66	18.993	
26	0.67	19.281	(Parapet)
30	0.7	20.444	(Shown for Interpolation)

T. 27.3-1

Check Rigidity	$n_u = 75/h$	Eqn 26.9-2
	$h = 24$ ft	
	$n_n = 1.747$ Hz Rigid	
	$G = 0.85$	

Building Criteria	h	L	B	h/L	L/B	Fig. 27.4-1
N/S Wind	24	75	120	0.32	0.625	
E/W Wind	24	120	75	0.2	1.6	

Parapet	$P_p = q_p(GC_{pm})$	27.4.5
	$q_p = 19.28$	
	$GC_{pm} = 1.5$ Windward	
	$GC_{pm} = -1$ Leeward	
	$P_p = 28.92$ psf Windward	
	$P_p = -19.28$ psf Leeward	
	$P_p = 48.20$ psf Total	

Pressures and Base Shear

N/S Wind									
Surface		q	G	Cp	Ext. P.	+ Int. P.	- Int. P.	Total (+) PSF	Total (-) PSF
Windward Wall	15	16.40	0.85	0.8	11.15	3.37	-3.37	7.79	14.52
	20	17.84	0.85	0.8	12.13	3.37	-3.37	8.77	15.50
	24	18.71	0.85	0.8	12.72	3.37	-3.37	9.35	16.09
Leeward Wall		18.71	0.85	-0.5	-7.95	3.37	-3.37	-11.32	-4.58
Total (+)				Total (-)					
Surface		Area	Pressure	Force (K)	Surface		Area	Pressure	Force (K)
Windward Wall	15	1800	7.79	14.02	Windward Wall	15	1800	14.52	26.14
	20	600	8.77	5.26		20	600	15.50	9.30
	24	480	9.35	4.49		25	480	16.09	7.72
Leeward Wall		2880	-11.32	-32.59	Leeward Wall		2880	-4.58	-13.20
Parapet		240	48.20	11.57	Parapet		240	48.20	11.57
Base Shear				67.93	Base Shear				67.93

Determine Design Spectral Response Acceleration	Location -	Memphis, TN	
	Coords. -	35.1066°N, 89.9786°W	
	Site Class -	D	
	$S_S =$	0.909	USGS Design Maps Applet
	$S_1 =$	0.319	
	$S_{MS} = F_a S_S$		Eqn. 11.4-1
	$F_a =$	1.14	T. 11.4-1
	$S_{MS} =$	1.03626	
	$S_{M1} = F_V S_1$		Eqn. 11.4-2
	$F_V =$	1.76	T. 11.4-2
$S_{M1} =$	0.56144		
$S_{DS} = (2/3) * S_{MS}$		Eqn. 11.4-3	
$S_{DS} =$	0.691		
$S_{D1} = (2/3) * S_{M1}$		Eqn. 11.4-4	
$S_{D1} =$	0.374		

Determine SDC	Building Category -	II	T. 1.5-1
	$I_E =$	1	T. 1.5-2
	Short Period	D	T. 11.6-1
	1-S Period	D	T. 11.6-2
	SDC =	D	

Approx. Fund. Period	$C_t =$	0.03	Eqn. 12.8-7
	$\alpha =$	0.75	
	$T_a = C_t h_n^\alpha$		

12 ft floor-to-floor height		
Stories	Height (h_n) (ft)	T_a (sec)
2	24	0.325

$T_L = 16$ s Fig. 22-13

Seismic
Response
Coefficients

$$C_s = S_{DS}/(R/I_e)$$

$$R = 8$$

$$I_E = 1$$

$$C_s = 0.086$$

Eqn. 12.8-2
Table 12.2-1
Table 12.2-1

Check Max
and Min

For $T \leq T_L$

$$C_{s,max} = S_{D1}/(T_a(R/I_e))$$

$$C_{s,max} = 0.144$$

Eqn. 12.8-3

$$C_{s,min} = 0.044S_{DS}I_e \geq 0.01$$

Eqn. 12.8-5

or $C_{s,min} = 0.5S_1/(R/I_e)$

Eqn. 12.8-6

$$C_{s,min} = 0.0304$$

or $C_{s,min} = 0.0199$

$C_{s,min}$	C_s	$C_{s,max}$	Use
0.030	0.086	0.144	0.086

Effective
Seismic
Weight

Plan Area	9000	sf
Floor Height	12	ft
Parapet	2	ft
Perimeter	390	ft

See Plans

Plan DL	110	psf
Roof DL	120	psf
Wall DL	20	psf

Dead Load
Calcs

$$W = \Sigma(\text{PlanDL} * \text{Area} + \text{WallDL} * \text{Height} * \text{Perimeter})$$

Level	Plan Wt (k)	Wall Wt (k)	Floor Total (k)
Roof	1080	62	1142
2	990	47	1037
Building Total			2179 k

Seismic Base
Shear

$$V = C_s W$$

Eqn. 12.8-1

$$C_s = 0.086$$

$$W = 2179 \text{ k}$$

$$V = 188 \text{ k}$$

Vertical
Distribution
2 Stories

$$F_x = C_{vx} V$$

$$V = 188 \text{ k}$$

Eqn 12.8-11

$$C_{vx} = w_x h_x^k / (\Sigma w_i h_i^k)$$

$$k = 1$$

Eqn 12.8-12

Level	h_x (ft)	h_x^k (ft)	W_x (k)	$h_x^k W_x$	C_{vx}	F_x (k)	V_x (k)
Roof	24	24.0	1142	27418	0.688	129	129
2	12	12.0	1037	12442	0.312	59	188
39859					1.000	188	

Vertical
Distribution

Level	F_x (k)
2 Story	
Roof	129
2	59

Rigidity

Each principal direction has four EBFs, so Center of Rigidity is geometrically centered in plan. Assume Center of Mass is geometrically centered in plan.

Torsional
Rigidity

$$J = \sum R d^2$$

$$R_{\text{Rel,long}} = 1 \text{ (k/in)}$$

$$R_{\text{Rel,trans}} = 1 \text{ (k/in)}$$

$$d_{\text{long}} = 60 \text{ ft}$$

$$d_{\text{trans}} = 37.5 \text{ ft}$$

$$J = 20025 \text{ k-ft}^2/\text{in}$$

Direct
Shear

$$V_D = (R_x/R_T) * F_x$$

Level	F_x (k)	R_x (k/in)	V_D (k)
Roof	129	2	65
2	59	2	30
	$R_T =$	4	

Eccentric
Shear

$$e_{\text{acc}} = +/- 0.05L$$

12.8.4.2

$$V_T = [V_x R_x (e + e_{\text{acc}})] / J$$

$$x_R = 60 \text{ ft}$$

$$e = 0 \text{ ft}$$

$$e_{\text{acc}} = 6 \text{ ft}$$

$$R_x = 2 \text{ (k/in)}$$

Level	F_x (k)	V'_x (k)
Roof	129	4.64
2	59	2.12

Total Shear
Along Frame
Line

$$V_T = V_D + V'_x$$

Level	V_T (k)
Roof	69
2	31

Appendix B – Load Combinations

Member RL

$P_D =$	11.8	k	$V_D =$	3.9	k	$M_D =$	12.6	k-ft
$P_L =$	0	k	$V_L =$	0	k	$M_L =$	0	k-ft
$P_{QE} =$	17.3	k	$V_{QE} =$	18	k	$M_{QE} =$	36.1	k-ft
$P_S =$	0.9	k	$V_S =$	0.3	k	$M_S =$	0.9	k-ft

$$(1.2 + 0.2S_{DS})D + \rho QE + 0.5L + 0.2S$$

$S_{DS} =$	0.691
$\rho =$	1

$P_u =$	33.4	k	$P_{nt} =$	16.0	k
$V_u =$	23.3	k	$P_{lt} =$	17.3	k
$M_u =$	53.2	k-ft	$M_{nt} =$	17.0	k-ft
			$M_{lt} =$	36.1	k-ft

Member 2L

$P_D =$	0.6	k	$V_D =$	4	k	$M_D =$	14.9	k-ft
$P_L =$	7	k	$V_L =$	2.4	k	$M_L =$	7.5	k-ft
$P_{QE} =$	7.7	k	$V_{QE} =$	26	k	$M_{QE} =$	52.2	k-ft
$P_S =$	0.9	k	$V_S =$	0	k	$M_S =$	0	k-ft

$$(1.2 + 0.2S_{DS})D + \rho QE + 0.5L + 0.2S$$

$S_{DS} =$	0.691
$\rho =$	1

$P_u =$	12.3	k	$P_{nt} =$	4.5	k
$V_u =$	32.6	k	$P_{lt} =$	7.7	k
$M_u =$	75.9	k-ft	$M_{nt} =$	23.7	k-ft
			$M_{lt} =$	52.2	k-ft

Member 2B

$P_D = 11.9 \text{ k}$ $P_L = 0 \text{ k}$ $P_{QE} = 32.7 \text{ k}$ $P_S = 0.9 \text{ k}$	$V_D = 7.8 \text{ k}$ $V_L = 4.8 \text{ k}$ $V_{QE} = 4 \text{ k}$ $V_S = 0 \text{ k}$	$M_D = 16 \text{ k-ft}$ $M_L = 9.5 \text{ k-ft}$ $M_{QE} = 35 \text{ k-ft}$ $M_S = 0 \text{ k-ft}$
---	---	---

Unamplified

$$(1.2 + 0.2S_{DS})D + \rho QE + 0.5L + 0.2S$$

$$S_{DS} = 0.691$$

$$\rho = 1$$

$P_u =$	49	k
$V_u =$	17	k
$M_u =$	61	k-ft

$P_D = 11.9 \text{ k}$ $P_L = 0 \text{ k}$ $P_E = 311 \text{ k}$ $P_S = 0.9 \text{ k}$	$V_D = 7.8 \text{ k}$ $V_L = 4.8 \text{ k}$ $V_E = 38 \text{ k}$ $V_S = 0 \text{ k}$	$M_D = 16 \text{ k-ft}$ $M_L = 9.5 \text{ k-ft}$ $M_E = 333 \text{ k-ft}$ $M_S = 0 \text{ k-ft}$
---	---	---

Amplified

$$(1.2 + 0.2S_{DS})D + \rho QE + 0.5L + 0.2S$$

$$S_{DS} = 0.691$$

$$\rho = 1$$

$P_u =$	327	k	$P_{nt} =$	16	k
$V_u =$	51	k	$P_{lt} =$	311	k
$M_u =$	359	k-ft	$M_{nt} =$	26	k-ft
			$M_{lt} =$	333	k-ft

Member RB

$P_D =$	0	k	$V_D =$	7.8	k	$M_D =$	15.6	k-ft
$P_L =$	0	k	$V_L =$	0	k	$M_L =$	0	k-ft
$P_{QE} =$	34.5	k	$V_{QE} =$	2.7	k	$M_{QE} =$	25	k-ft
$P_S =$	0	k	$V_S =$	0.8	k	$M_S =$	1.2	k-ft

Unamplified

$$(1.2 + 0.2S_{DS})D + \rho QE + 0.5L + 0.2S$$

$$S_{DS} = 0.691$$

$$\rho = 1$$

$P_u =$	35	k
$V_u =$	13	k
$M_u =$	46	k-ft

$P_D =$	0	k	$V_D =$	7.8	k	$M_D =$	15.6	k-ft
$P_L =$	0	k	$V_L =$	0	k	$M_L =$	0	k-ft
$P_E =$	474	k	$V_E =$	37	k	$M_E =$	343	k-ft
$P_S =$	0	k	$V_S =$	0.8	k	$M_S =$	1.2	k-ft

Amplified

$$(1.2 + 0.2S_{DS})D + \rho QE + 0.5L + 0.2S$$

$$S_{DS} = 0.691$$

$$\rho = 1$$

$P_u =$	474	k	$P_{nt} =$	0	k
$V_u =$	48	k	$P_{lt} =$	474	k
$M_u =$	364	k-ft	$M_{nt} =$	21	k-ft
			$M_{lt} =$	343	k-ft

Member 2BR

$P_D =$	19.5	k	$V_D =$	0.4	k	$M_D =$	2.6	k-ft
$P_L =$	0	k	$V_L =$	0	k	$M_L =$	0	k-ft
$P_{QE} =$	27	k	$V_{QE} =$	0.6	k	$M_{QE} =$	11	k-ft
$P_S =$	1.4	k	$V_S =$	0	k	$M_S =$	0.2	k-ft

Unamplified

$$(1.2 + 0.2S_{DS})D + \rho QE + 0.5L + 0.2S$$

$$S_{DS} = \frac{0.691}{1}$$

$P_u =$	54	k
$V_u =$	1	k
$M_u =$	15	k-ft

$P_D =$	19.5	k	$V_D =$	0.4	k	$M_D =$	2.6	k-ft
$P_L =$	0	k	$V_L =$	0	k	$M_L =$	0	k-ft
$P_E =$	371	k	$V_E =$	8	k	$M_E =$	151	k-ft
$P_S =$	1.4	k	$V_S =$	0	k	$M_S =$	0.2	k-ft

Amplified

$$(1.2 + 0.2S_{DS})D + \rho QE + 0.5L + 0.2S$$

$$S_{DS} = \frac{0.691}{1}$$

$P_u =$	398	k	$P_{nt} =$	26	k
$V_u =$	9	k	$P_{lt} =$	371	k
$M_u =$	155	k-ft	$M_{nt} =$	4	k-ft
			$M_{lt} =$	151	k-ft

Member 1BR

$P_D = 20.9$ k	$V_D = 0.7$ k	$M_D = 3.4$ k-ft
$P_L = 11.5$ k	$V_L = 0.1$ k	$M_L = 2.2$ k-ft
$P_{QE} = 38.8$ k	$V_{QE} = 1.1$ k	$M_{QE} = 16.9$ k-ft
$P_S = 0$ k	$V_S = 0$ k	$M_S = 0$ k-ft

Unamplified

$$(1.2 + 0.2S_{DS})D + \rho QE + 0.5L + 0.2S$$

$$S_{DS} = \frac{0.691}{1}$$

$P_u = 73$	k
$V_u = 2$	k
$M_u = 23$	k-ft

$P_D = 20.9$ k	$V_D = 0.7$ k	$M_D = 3.4$ k-ft
$P_L = 11.5$ k	$V_L = 0.1$ k	$M_L = 2.2$ k-ft
$P_E = 369$ k	$V_E = 10$ k	$M_E = 161$ k-ft
$P_S = 0$ k	$V_S = 0$ k	$M_S = 0$ k-ft

Amplified

$$(1.2 + 0.2S_{DS})D + \rho QE + 0.5L + 0.2S$$

$$S_{DS} = \frac{0.691}{1}$$

$P_u = 403$	k	$P_{nt} = 34$	k
$V_u = 11$	k	$P_{lt} = 369$	k
$M_u = 167$	k-ft	$M_{nt} = 6$	k-ft
		$M_{lt} = 161$	k-ft

Redundancy Load Combination

$P_D = 31.1$ k	$V_D = 0$ k	$M_D = 0$ k-ft
$P_L = 0$ k	$V_L = 0$ k	$M_L = 0$ k-ft
$P_{QE} = 2.7$ k	$V_{QE} = 0$ k	$M_{QE} = 0$ k-ft
$P_S = 0.6$ k	$V_S = 0$ k	$M_S = 0$ k-ft

$$(1.2 + 0.2S_{DS})D + \rho QE + 0.5L + 0.2S$$

$S_{DS} =$	0.691
$\rho =$	1

$P_u =$	44	k
$V_u =$	0	k
$M_u =$	0	k-ft

Overstrength Load Combination

$P_D = 31.1$ k	$V_D = 0$ k	$M_D = 0$ k-ft
$P_L = 0$ k	$V_L = 0$ k	$M_L = 0$ k-ft
$P_{QE} = 2.7$ k	$V_{QE} = 0$ k	$M_{QE} = 0$ k-ft
$P_S = 0.6$ k	$V_S = 0$ k	$M_S = 0$ k-ft

$$(1.2 + 0.2S_{DS})D + \Omega QE + 0.5L + 0.2S$$

$S_{DS} =$	0.691
$\Omega =$	2

$P_u = 47$ k	$P_{nt} = 42$ k
$V_u = 0$ k	$P_{lt} = 5$ k
$M_u = 0$ k-ft	$M_{nt} = 0$ k-ft
	$M_{lt} = 0$ k-ft

Overstrength with Fully Yielded Link Force

$$\begin{array}{l}
 P_D = \\
 P_L = \\
 P_E = \\
 P_S =
 \end{array}
 \begin{array}{|c|}
 \hline
 31.1 \\
 \hline
 0 \\
 \hline
 218 \\
 \hline
 0.6 \\
 \hline
 \end{array}
 \begin{array}{l}
 \text{k} \\
 \text{k} \\
 \text{k} \\
 \text{k}
 \end{array}$$

$$\begin{array}{l}
 V_D = \\
 V_L = \\
 V_{QE} = \\
 V_S =
 \end{array}
 \begin{array}{|c|}
 \hline
 0 \\
 \hline
 0 \\
 \hline
 0 \\
 \hline
 0 \\
 \hline
 \end{array}
 \begin{array}{l}
 \text{k} \\
 \text{k} \\
 \text{k} \\
 \text{k}
 \end{array}$$

$$\begin{array}{l}
 M_D = \\
 M_L = \\
 M_{QE} = \\
 M_S =
 \end{array}
 \begin{array}{|c|}
 \hline
 0 \\
 \hline
 0 \\
 \hline
 0 \\
 \hline
 0 \\
 \hline
 \end{array}
 \begin{array}{l}
 \text{k-ft} \\
 \text{k-ft} \\
 \text{k-ft} \\
 \text{k-ft}
 \end{array}$$

$$\begin{aligned}
 P: & (1.2 + 0.2S_{DS})D + 1.0E + 0.5L + 0.2S \\
 V \text{ and } M: & (1.2 + 0.2S_{DS})D + \Omega QE + 0.5L + 0.2S
 \end{aligned}$$

$$\begin{array}{l}
 S_{DS} = \\
 \Omega =
 \end{array}
 \begin{array}{|c|}
 \hline
 0.691 \\
 \hline
 2 \\
 \hline
 \end{array}$$

$$\begin{array}{l}
 P_u = \\
 V_u = \\
 M_u =
 \end{array}
 \begin{array}{|c|}
 \hline
 260 \\
 \hline
 0 \\
 \hline
 0 \\
 \hline
 \end{array}
 \begin{array}{l}
 \text{k} \\
 \text{k} \\
 \text{k-ft}
 \end{array}$$

$$\begin{array}{l}
 P_{nt} = \\
 P_{lt} = \\
 M_{nt} = \\
 M_{lt} =
 \end{array}
 \begin{array}{|c|}
 \hline
 42 \\
 \hline
 218 \\
 \hline
 0 \\
 \hline
 0 \\
 \hline
 \end{array}
 \begin{array}{l}
 \text{k} \\
 \text{k} \\
 \text{k-ft} \\
 \text{k-ft}
 \end{array}$$

Member 1C

Redundancy Load Combination

$P_D =$	76.6	k
$P_L =$	20	k
$P_{QE} =$	14.3	k
$P_S =$	2	k

$V_D =$	0	k
$V_L =$	0	k
$V_{QE} =$	0	k
$V_S =$	0	k

$M_D =$	0	k-ft
$M_L =$	0	k-ft
$M_{QE} =$	0	k-ft
$M_S =$	0	k-ft

$$(1.2 + 0.2S_{DS})D + \rho QE + 0.5L + 0.2S$$

$S_{DS} =$	0.691
$\rho =$	1.3

$P_u =$	132	k
$V_u =$	0	k
$M_u =$	0	k-ft

Overstrength Load Combination

$P_D =$	76.6	k
$P_L =$	20	k
$P_{QE} =$	14.3	k
$P_S =$	2	k

$V_D =$	0	k
$V_L =$	0	k
$V_{QE} =$	0	k
$V_S =$	0	k

$M_D =$	0	k-ft
$M_L =$	0	k-ft
$M_{QE} =$	0	k-ft
$M_S =$	0	k-ft

$$(1.2 + 0.2S_{DS})D + \Omega QE + 0.5L + 0.2S$$

$S_{DS} =$	0.691
$\Omega =$	2

$P_u =$	142	k	$P_{nt} =$	113	k
$V_u =$	0	k	$P_{lt} =$	29	k
$M_u =$	0	k-ft	$M_{nt} =$	0	k-ft
			$M_{lt} =$	0	k-ft

Fully Yielded Link Load Combination

$P_D =$	76.6	k
$P_L =$	20	k
$P_E =$	435	k
$P_S =$	2	k

$V_D =$	0	k
$V_L =$	0	k
$V_{QE} =$	0	k
$V_S =$	0	k

$M_D =$	0	k-ft
$M_L =$	0	k-ft
$M_{QE} =$	0	k-ft
$M_S =$	0	k-ft

P: $(1.2 + 0.2S_{DS})D + 1.0E + 0.5L + 0.2S$
V and M: $(1.2 + 0.2S_{DS})D + \Omega QE + 0.5L + 0.2S$

$S_{DS} =$	0.691
$\Omega =$	2

$P_u =$	548	k
$V_u =$	0	k
$M_u =$	0	k-ft

$P_{nt} =$	113	k
$P_{lt} =$	435	k
$M_{nt} =$	0	k-ft
$M_{lt} =$	0	k-ft

Appendix C – EBF Member Design

Allowable Story Drift

Cat II SDC D so Divide by redundancy factor

ASCE 7-10 12.12

$$\Delta_a = \frac{0.025 * h_{sx} / \rho}{\rho = \frac{1}{12} \text{ ft}}$$

$$\Delta_a = 3.60 \text{ in}$$

ASCE 7-10 T. 12.12-1
ASCE 7-10 S. 12.12.1.1

Design Earthquake Deflection

$$\delta_x = C_d \delta_{xe} / I$$

$$C_d = \frac{4}{1}$$

$$\delta_x = 4 * \delta_{xe}$$

δ_{xe} from RISA 3D service load analysis

ASCE 7-10 Eqn. 12.8-15
ASCE 7-10 T. 12.2-1
ASCE 7-10 T. 1.5-2
AISC 358-10 S. 5.8

Level	δ_{xe}	δ_x	Δ	Δ_a	Check
Roof	0.059	0.24	0.11	3.60	OK
2	0.031	0.12	0.12	3.60	OK

Level	δ_{xe}	δ_{xie}	Δ
Roof	0.059	0.18	0.08
2	0.031	0.09	0.09

Second Order B₂

$$B_2 = 1 / (1 - P_{\text{story}} / P_{\text{story}}) \geq 1$$

AISC 360-10 A-8-6

$$P_{\text{story}} = R_M (HL / \Delta H)$$

AISC 360-10 A-8-7

Story	RM	H	L	dH	P _{story}
2	1	34.5	144	0.236	21051
1	1	15.5	144	0.124	18000

Story	D (k)			Type	Count
	Corner	Edge	Int		
2	23	45	90	Corner	4
1	44	87	173	Edge	10
				Int	6

$$(1 + 1.4 \text{SDS})D + 0.7QE$$

ASCE 7-10

Story	D _{total}	P _{story}	Story	B ₂
2	1082	1187	2	1.06
1	2084	2286	1	1.15

Member RL OK

P_u (k)	V_u (k)	M_u (k-ft)
33.4	23.3	53.2

RISA 3D Outputs

Section W12X96

d (in)	t_w (in)	A_g (in ²)	t_f (in)	e (in)	Δ_p (in)
12.7	0.55	28.2	0.9	48	0.08
b_f (in)	Z_x (in ³)	E (ksi)	Fy (ksi)	h (ft)	L (ft)
12.2	147	29000	50	12	25
I_x (in ⁴)					
833					

AISC 360-10

T. 1-1

T. 3-2

Check Geometry

Brace-Link work point at the end or within link? OK
 $b_{f,link} > b_{f,brace}$ OK

Check Slenderness (Highly Ductile)

341-10 D1

$$\lambda_f = b_f / 2t_f$$

$$\lambda_f = 6.78$$

$$\lambda_{ps} = 0.3\sqrt{E/F_y}$$

$$\lambda_{ps} = 7.22$$

AISC 341-10

T. D1.1

$$\lambda_f = 6.78 < \lambda_{ps} = 7.22$$

OK

$$\lambda_w = d/t_w$$

$$\lambda_w = 23.09$$

$$C_a = P_u / \phi_c P_y$$

$$C_a = 0.026$$

T. D1.1

$$\lambda_{ps} = 2.45\sqrt{E/F_y}(1-0.93C_a)$$

$$\lambda_{ps} = 57.56$$

T. D1.1

$$\lambda_w = 23.09 < \lambda_{ps} = 57.56$$

OK

Determine Shear Strength

341-10 F3.5b(2)

$$P_u/P_y = 0.024$$

$$V_p = 0.6F_y(d-2t_f)t_w$$

Eqn F3-2,3

$$V_p = 180 \text{ k}$$

$$M_p = F_y Z$$

Eqn F3-8,9

$$M_p = 7350 \text{ k-in}$$

$$\phi V_n = \phi V_p \leq \phi 2M_p/e \quad \phi = 0.9$$

$$\phi V_p = 162 \text{ k}$$

$$\phi 2M_p/e = 276 \text{ k}$$

$$\phi V_n = 162 \text{ k}$$

$$V_u = 23.3 < \phi V_n = 162$$

OK

Check Link Length

$$P_u/P_y = 0.024 \leq 0.15$$

Link Length Not Limited

$$\rho' = (P_u/P_y)/(V_u/V_y)$$

$$\rho' = 0.18$$

$$e \leq \text{No Limit}$$

$$e \leq \text{No Limit in}$$

OK

Check Link Rotation Angle

341-10 F3.4a

$$X = eV_p/M_p$$

$$X = 1.17 \quad \therefore \text{Shear Link}$$

$$\gamma_p \leq 0.080 \text{ rad}$$

F3.4a

$$\gamma_p \approx L\Delta_p/eh$$

F. C-F3.4a

$$\gamma_p = 0.004 \text{ rad}$$

$$\gamma_p = 0.004 < 0.08$$

OK

$$\text{Max } \Delta_p = 1.84 \text{ in} \quad 0.08$$

Link End Top and Bottom Lateral Bracing

$$R_u = 0.06R_y F_y Z/h_0$$

$$R_u = 41 \text{ k}$$

Eqn D1-7/G2-1

Consider Second-Order Effects

$$L_b = 4 \text{ ft}$$

$$B_1 = C_m / (1 - \alpha P_r / P_{e1}) \geq 1$$

$$\alpha = 1 \quad (\text{LRFD})$$

$$C_m = 1 \quad (\text{Transverse Loading})$$

$$P_r = P_u = 33.4 \text{ k} \quad (\text{First Order Estimate})$$

$$P_{e1} = \pi^2 EI / (K_1 L)^2$$

$$EI = 167756.9 \text{ k-ft}^2$$

$$K_1 = 1 \quad (\text{Assumed})$$

$$L = 4 \text{ ft}$$

$$P_{e1} = 103481 \text{ k}$$

$$B_1 = 1.000 = 1.000$$

$$B_2 = 1.06$$

310-10 Eqn A-8-3

310-10 Eqn A-8-5

$$P_{nt} = 16 \text{ k}$$

$$M_{nt} = 17 \text{ k-ft}$$

$$P_{it} = 17.3 \text{ k}$$

$$M_{it} = 36.1 \text{ k-ft}$$

$$M_r = B_1 M_{nt} + B_2 M_{it}$$

$$P_r = P_{nt} + B_2 P_{it}$$

$$M_r = 55 \text{ k-ft}$$

$$P_r = 34 \text{ k}$$

Check Combined Loading

$$KL_y = L_{bx} = 4 \text{ ft} \quad \text{W12X96}$$

$$p = 0.88 \times 10^{-3} (\text{k-ft})^{-1}$$

$$b_x = 1.61 \times 10^{-3} (\text{k-ft})^{-1}$$

360-10 T. 6-1

$$P_r / P_c = p P_r = 0.030 < 0.2$$

$$(8/9)(M_{rx} / M_{cx}) = b_x M_{rx} / R_y$$

$$b_x M_{rx} = 0.089$$

$$.5pP_r + (9/8)(b_x M_{rx}) = 0.115$$

OK

360-10 Eqn 6-1/2

Required Stiffeners

AISC 341-10
Sec. F3.5b(4)

Double Sided, Full-Depth End Stiffeners

$$w_{\min} = (b_f - 2t_w)/2$$

$$w_{\min} = 5.55 \text{ in}$$

$$t_{\min} = 0.75t_w \geq 0.375$$

$$t_{\min} = 0.41 \text{ in}$$

USE $t = 1/2 \text{ in}$
 $w = 5 \ 3/4 \text{ in}$

Intermediate Stiffeners

If Shear Link

$$s = 0.08 \text{ rad}$$

$$s = 30t_w - d/5 \quad 52t_w - d/5$$

$$s = 14.0 \quad 26.1 \text{ in}$$

$$\gamma_p = 0.004 \text{ rad}$$

$$s_{\max} = 26.1 \text{ in} \quad (\text{interpolation})$$

If Flexure Link

$$s_{\max} = 1.5b_f \quad \text{from link ends}$$

$$s_{\max} = 18.3 \text{ in}$$

If Intermediate Link

both shear and flexure requirements

RESULT Shear Link

$$s_{\max} = 26.1 \text{ in}$$

Is $d < 25 \text{ in}$?

Yes - Single Sided

$$t_{\min} = t_w \geq 0.375$$

$$t_{\min} = 0.55 \text{ in}$$

$$w_{\min} = (bf/2) - tw$$

$$w_{\min} = 5.55 \text{ in}$$

sides = Single

USE s = 26 in
 t = 5/8 in
 w = 5 3/4 in

Member 2L OK

P_u (k)	V_u (k)	M_u (k-ft)
12.3	32.6	75.9

RISA 3D Outputs

Section W12X96

d (in)	t_w (in)	A_g (in ²)	t_f (in)	e (in)	Δ_p (in)
12.7	0.55	28.2	0.9	48	0.09
b_f (in)	Z_x (in ³)	E (ksi)	Fy (ksi)	h (ft)	L (ft)
12.2	147	29000	50	12	25
I_x (in ⁴)					
833					

AISC 360-10

T. 1-1

T. 3-2

Check Geometry

Brace-Link work point at the end or within link? OK
 $b_{f,link} > b_{f,brace}$? OK

Check Slenderness (Highly Ductile)

341-10 D1

$$\lambda_f = b_f / 2t_f$$

$$\lambda_f = 6.78$$

$$\lambda_{ps} = 0.3 \sqrt{E/F_y}$$

$$\lambda_{ps} = 7.22$$

AISC 341-10

T. D1.1

$$\lambda_f = 6.78 < \lambda_{ps} = 7.22$$

OK

$$\lambda_w = d/t_w$$

$$\lambda_w = 23.09$$

$$C_a = P_u / \phi_c P_y$$

$$C_a = 0.010$$

T. D1.1

$$\lambda_{ps} = 2.45 \sqrt{E/F_y} (1 - 0.93 C_a)$$

$$\lambda_{ps} = 58.47$$

T. D1.1

$$\lambda_w = 23.09 < \lambda_{ps} = 58.47$$

OK

Determine Shear Strength

341-10 F3.5b(2)

$$P_u/P_y = 0.009$$

$$V_p = 0.6F_y(d-2t_f)t_w$$

Eqn F3-2,3

$$V_p = 180 \text{ k}$$

$$M_p = F_y Z$$

Eqn F3-8,9

$$M_p = 7350 \text{ k-in}$$

$$\phi V_n = \phi V_p \leq \phi 2M_p/e \quad \phi = 0.9$$

$$\phi V_p = 162 \text{ k}$$

$$\phi 2M_p/e = 276 \text{ k}$$

$$\phi V_n = 162 \text{ k}$$

$$V_u = 32.6 < \phi V_n = 162$$

OK

Check Link Length

$$P_u/P_y = 0.009 \leq 0.15$$

Link Length Not Limited

$$\rho' = (P_u/P_y)/(V_u/V_y)$$

$$\rho' = 0.05$$

$$e \leq \text{No Limit}$$

$$e \leq \text{No Limit in}$$

OK

Check Link Rotation Angle

341-10 F3.4a

$$X = eV_p/M_p$$

$$X = 1.17 \quad \therefore \text{Shear Link}$$

$$\gamma_p \leq 0.080 \text{ rad}$$

F3.4a

$$\gamma_p \approx L\Delta_p/eh$$

F. C-F3.4a

$$\gamma_p = 0.004 \text{ rad}$$

$$\gamma_p = 0.004 < 0.08$$

OK

$$\text{Max } \Delta_p = 1.84 \text{ in} \quad 0.09$$

Link End Top and Bottom Lateral Bracing

$$R_u = 0.06R_y F_y Z/h_0 \quad \text{Eqn D1-7/G2-1}$$
$$R_u = 41 \quad \text{k}$$

Consider Second-Order Effects

$$L_b = 4 \quad \text{ft}$$

$$B_1 = C_m / (1 - \alpha P_r / P_{e1}) \geq 1 \quad \text{310-10 Eqn A-8-3}$$

$$\alpha = 1 \quad (\text{LRFD})$$

$$C_m = 1 \quad (\text{Transverse Loading})$$

$$P_r = P_u = 12.3 \quad \text{k} \quad (\text{First Order Estimate})$$

$$P_{e1} = \pi^2 EI / (K_1 L)^2 \quad \text{310-10 Eqn A-8-5}$$

$$EI = 167756.9 \quad \text{k-ft}^2$$

$$K_1 = 1 \quad (\text{Assumed})$$

$$L = 4 \quad \text{ft}$$

$$P_{e1} = 103481 \quad \text{k}$$

$$B_1 = 1.000 = 1.000$$

$$B_2 = 1.06$$

$$P_{nt} = 4.5 \quad \text{k}$$

$$M_{nt} = 23.7 \quad \text{k-ft}$$

$$P_{lt} = 7.7 \quad \text{k}$$

$$M_{lt} = 52.2 \quad \text{k-ft}$$

$$M_r = B_1 M_{nt} + B_2 M_{lt}$$

$$P_r = P_{nt} + B_2 P_{lt}$$

$$M_r = 79 \quad \text{k-ft}$$

$$P_r = 13 \quad \text{k}$$

Check Combined Loading

$$KL_y = L_{bx} = 4 \quad \text{ft} \quad \text{W12X96}$$

$$p = 0.88 \times 10^{-3} \quad (\text{k-ft})^{-1}$$

360-10 T. 6-1

$$b_x = 1.61 \times 10^{-3} \quad (\text{k-ft})^{-1}$$

$$P_r / P_c = p P_r = 0.011 < 0.2$$

$$(8/9)(M_{rx} / M_{cx}) = b_x M_{rx} / R_y$$

$$b_x M_{rx} = 0.127$$

$$.5pP_r + (9/8)(b_x M_{rx}) = 0.149$$

360-10 Eqn 6-1/2

OK

Required Stiffeners

AISC 341-10
Sec. F3.5b(4)

Double Sided, Full-Depth End Stiffeners

$$w_{\min} = (b_f - 2t_w)/2$$

$$w_{\min} = 5.55 \text{ in}$$

$$t_{\min} = 0.75t_w \geq 0.375$$

$$t_{\min} = 0.41 \text{ in}$$

USE $t = 1/2 \text{ in}$
 $w = 5 \ 3/4 \text{ in}$

Intermediate Stiffeners

If Shear Link

$$s = \frac{0.08}{30t_w - d/5} = \frac{0.02}{52t_w - d/5} \text{ rad}$$

$$s = \frac{14.0}{26.1} \text{ in}$$

$$\gamma_p = 0.004 \text{ rad}$$

$$s_{\max} = 26.1 \text{ in (interpolation)}$$

If Flexure Link

$$s_{\max} = 1.5bf \text{ from link ends}$$

$$s_{\max} = 18.3 \text{ in}$$

If Intermediate Link

both shear and flexure requirements

RESULT Shear Link

$$s_{\max} = 26.1 \text{ in}$$

Is $d < 25 \text{ in}$?

Yes - Single Sided

$$t_{\min} = t_w \geq 0.375$$

$$t_{\min} = 0.55 \text{ in}$$

$$w_{\min} = (bf/2) - tw$$

$$w_{\min} = 5.55 \text{ in}$$

USE

$$\begin{aligned} \text{sides} &= \text{Single} \\ s &= 26 \text{ in} \\ t &= 5/8 \text{ in} \\ w &= 5 \ 3/4 \text{ in} \end{aligned}$$

Member RB OK

P_D (k)	P_L (k)	P_{QE} (k)	P_S (k)
0	0	34.5	0
V_D (k)	V_L (k)	V_{QE} (k)	V_S (k)
7.8	0	2.7	0.8
M_D (k-ft)	M_L (k-ft)	M_{QE} (k-ft)	M_S (k-ft)
15.6	0	25	1.2

RISA 3D Outputs

Section W12X96

d (in)	t_w (in)	A_g (in ²)	t_f (in)	e (in)	Δ_p (in)
12.7	0.55	28.2	0.9	48	0.11
b_f (in)	Z_x (in ³)	E (ksi)	F_y (ksi)	h (ft)	L (ft)
12.2	147	29000	50	12	25
I_x (in ⁴)	R_y				
833	1.1				

AISC 360-10

T. 1-1

T. 3-2

Determine Factored Loads (Based on Link Shear Overstrength)

$$V_{QE} = 18 \text{ k (Link)}$$

$$V_p = 180 \text{ k (Link)}$$

$$1.25R_y V_n = 247 \text{ k (Amplified Link Shear Force)}$$

$$1.25R_y V_n / V_{QE} = 13.74 \text{ (Overstrength Factor)}$$

$$M_E = 343 \text{ k-ft}$$

$$P_E = 474 \text{ k (in beam due to link)}$$

$$V_E = 37 \text{ k}$$

P_u (k)	V_u (k)	M_u (k-ft)
474	48	364

From Load Calculations

Check Slenderness (Moderately Ductile)

341-10 D1

$$\lambda_f = b_f / 2t_f$$

$$\lambda_f = 6.78$$

$$\lambda_{ps} = 0.38 \sqrt{E/F_y}$$

$$\lambda_{ps} = 9.15$$

AISC 341-10

T. D1.1

$$\lambda_f = 6.78 < \lambda_{ps} = 9.15$$

OK

$$\lambda_w = d/tw$$

$$\lambda_w = 23.09$$

$$C_a = P_u / \phi_c P_y \quad \text{T. D1.1}$$

$$C_a = 0.374$$

$$\lambda_{ps} = 1.12 \sqrt{E/F_y} (2.33 - C_a) \geq 1.49 \sqrt{E/F_y} \quad \text{T. D1.1}$$

$$\lambda_{ps} = 52.77$$

$$\lambda_w = 23.09 < \lambda_{ps} = 52.77$$

OK

Consider Second-Order Effects

$$L_b = (L - e)/2 \quad (\text{Conservative})$$

$$L_b = 10.5 \quad \text{ft}$$

$$B_1 = C_m / (1 - \alpha P_r / P_{e1}) \geq 1 \quad \text{310-10 Eqn A-8-3}$$

$$\alpha = 1 \quad (\text{LRFD})$$

$$C_m = 1 \quad (\text{Transverse Loading})$$

$$P_r = P_u = 474 \quad \text{k} \quad (\text{First Order Estimate})$$

$$P_{e1} = \pi^2 EI / (K_1 L)^2 \quad \text{310-10 Eqn A-8-5}$$

$$EI = 167756.9 \quad \text{k-ft}^2$$

$$K_1 = 1 \quad (\text{Assumed})$$

$$L = 10.5 \quad \text{ft}$$

$$P_{e1} = 15018 \quad \text{k}$$

$$B_1 = 1.033 = 1.033$$

$$B_2 = 1.06$$

$$P_{nt} = 0 \quad \text{k}$$

$$M_{nt} = 21 \quad \text{k-ft}$$

$$P_{lt} = 474 \quad \text{k}$$

$$M_{lt} = 343 \quad \text{k-ft}$$

$$M_r = B_1 M_{nt} + B_2 M_{lt}$$

$$P_r = P_{nt} + B_2 P_{lt}$$

$$M_r = 385 \quad \text{k-ft}$$

$$P_r = 502.3164 \quad \text{k}$$

Check Combined Loading

$$KL_y = L_{bx} = 10.5 \text{ ft} \quad \text{W12X96}$$

$$p = 0.901 \times 10^{-3} \text{ (k-ft)}^{-1}$$

360-10 T. 6-1

$$b_x = 1.61 \times 10^{-3} \text{ (k-ft)}^{-1}$$

$$P_r/P_c = pP_r/R_y = 0.411 \geq 0.2$$

$$(8/9)(M_{rx}/M_{cx}) = b_x M_{rx}/R_y$$

$$b_x M_{rx}/R_y = 0.564$$

$$pPr + B_x M_{rx} = 0.975$$

360-10 Eqn 6-1/2

OK

Member 2B OK

P_D (k)	P_L (k)	P_{QE} (k)	P_S (k)
11.9	0	32.7	0.9
V_D (k)	V_L (k)	V_{QE} (k)	V_S (k)
7.8	4.8	4	0
M_D (k-ft)	M_L (k-ft)	M_{QE} (k-ft)	M_S (k-ft)
16	9.5	35	0

RISA 3D Outputs

Section W12X96

d (in)	t_w (in)	A_g (in ²)	t_f (in)	e (in)	Δ_p (in)
12.7	0.55	28.2	0.9	48	0.12
b_f (in)	Z_x (in ³)	E (ksi)	F_y (ksi)	h (ft)	L (ft)
12.2	147	29000	50	12	25
I_x (in ⁴)	R_y				
833	1.1				

AISC 360-10

T. 1-1

T. 3-2

Determine Factored Loads (Based on Link Shear Overstrength)

$$V_{QE} = 26 \text{ k (Link)}$$

$$V_p = 180 \text{ k (Link)}$$

$$1.25R_y V_n = 247 \text{ k (Amplified Link Shear Force)}$$

$$1.25R_y V_n / V_{QE} = 9.51 \text{ (Overstrength Factor)}$$

$$M_E = 333 \text{ k-ft}$$

$$P_E = 311 \text{ k (in beam due to link)}$$

$$V_E = 38 \text{ k}$$

P_u (k)	V_u (k)	M_u (k-ft)
327	51	359

From Load Calculations

Check Slenderness (Moderately Ductile)

341-10 D1

$$\lambda_f = b_f / 2t_f$$

$$\lambda_f = 6.78$$

$$\lambda_{ps} = 0.38 \sqrt{E/F_y}$$

$$\lambda_{ps} = 9.15$$

AISC 341-10

T. D1.1

$$\lambda_f = 6.78 < \lambda_{ps} = 9.15$$

OK

$$\lambda_w = d/t_w$$

$$\lambda_w = 23.09$$

$$C_a = P_u / \phi_c P_y \quad \text{T. D1.1}$$

$$C_a = 0.258$$

$$\lambda_{ps} = 1.12 \sqrt{E/F_y} (2.33 - C_a) \geq 1.49 \sqrt{E/F_y} \quad \text{T. D1.1}$$

$$\lambda_{ps} = 55.90$$

$$\lambda_w = 23.09 < \lambda_{ps} = 55.90$$

OK

Consider Second-Order Effects

$$L_b = (L - e) / 2 \quad (\text{Conservative})$$

$$L_b = 10.5 \quad \text{ft}$$

$$B_1 = C_m / (1 - \alpha P_r / P_{e1}) \geq 1 \quad \text{310-10 Eqn A-8-3}$$

$$\alpha = 1 \quad (\text{LRFD})$$

$$C_m = 1 \quad (\text{Transverse Loading})$$

$$P_r = P_u = 327 \quad \text{k} \quad (\text{First Order Estimate})$$

$$P_{e1} = \pi^2 EI / (K_1 L)^2 \quad \text{310-10 Eqn A-8-5}$$

$$EI = 167756.9 \quad \text{k-ft}^2$$

$$K_1 = 1 \quad (\text{Assumed})$$

$$L = 10.5 \quad \text{ft}$$

$$P_{e1} = 15018 \quad \text{k}$$

$$B_1 = 1.022 = 1.022$$

$$B_2 = 1.15$$

$$P_{nt} = 16 \quad \text{k} \quad M_{nt} = 26 \quad \text{k-ft}$$

$$P_{lt} = 311 \quad \text{k} \quad M_{lt} = 333 \quad \text{k-ft}$$

$$M_r = B_1 M_{nt} + B_2 M_{lt}$$

$$M_r = 408 \quad \text{k-ft}$$

$$P_r = P_{nt} + B_2 P_{lt}$$

$$P_r = 372 \quad \text{k}$$

Check Combined Loading

$$KL_y = L_{bx} = 10.5 \text{ ft} \quad \text{W12X96}$$

$$p = 0.901 \times 10^{-3} \text{ (k-ft)}^{-1}$$

360-10 T. 6-1

$$b_x = 1.61 \times 10^{-3} \text{ (k-ft)}^{-1}$$

$$P_r/P_c = pP_r/R_y = 0.305 \geq 0.2$$

$$(8/9)(M_{rx}/M_{cx}) = b_x M_{rx}/R_y$$

$$b_x M_{rx}/R_y = 0.597$$

$$pPr + B_x M_{rx} = 0.902$$

360-10 Eqn 6-1/2

OK

Member 2BR

OK

RISA 3D Outputs

P_D (k)	P_L (k)	P_{QE} (k)	P_S (k)
19.5	0	27	1.4
V_D (k)	V_L (k)	V_{QE} (k)	V_S (k)
0.4	0	0.6	0
M_D (k-ft)	M_L (k-ft)	M_{QE} (k-ft)	M_S (k-ft)
2.6	0	11	0.2

Section

W10X88

AISC 360-10

T. 1-1

T. 3-2

d (in)	t_w (in)	A_g (in ²)	t_f (in)	e (in)	Δ_p (in)
10.8	0.605	26	0.99	48	0.11
b_f (in)	Z_x (in ³)	E (ksi)	F_y (ksi)	h (ft)	L (ft)
10.3	113	29000	50	12	25
I_x (in ⁴)	R_y				
534	1.1				

Determine Factored Loads

(Based on Link Shear Overstrength)

$$V_{QE} = 18 \text{ k} \quad (\text{Link Shear Force})$$

$$V_n = 180 \text{ k} \quad (\text{Link})$$

$$1.25R_y V_n = 247 \text{ k} \quad (\text{Amplified Link Shear Force})$$

$$1.25R_y V_n / V_{QE} = 13.74 \quad (\text{Overstrength Factor})$$

$$M_E = 151 \text{ k-ft}$$

$$P_E = 371 \text{ k} \quad (\text{in beam due to link})$$

$$V_E = 8 \text{ k}$$

P_u (k)	V_u (k)	M_u (k-ft)
398	9	155

From Load Calculations

Check Slenderness (Moderately Ductile)

341-10 D1

$$\lambda_f = b_f / 2t_f$$

$$\lambda_f = 5.20$$

$$\lambda_{ps} = 0.38 \sqrt{E/F_y}$$

$$\lambda_{ps} = 9.15$$

AISC 341-10

T. D1.1

$$\lambda_f = 5.20 < \lambda_{ps} = 9.15$$

OK

$$\lambda_w = d/tw$$

$$\lambda_w = 17.85$$

$$C_a = P_u / \phi_c P_y \quad \text{T. D1.1}$$

$$C_a = 0.340$$

$$\lambda_{ps} = 1.12 \sqrt{E/F_y} (2.33 - C_a) >= 1.49 \sqrt{E/F_y} \quad \text{T. D1.1}$$

$$\lambda_{ps} = 53.67$$

$$\lambda_w = 17.85 < \lambda_{ps} = 53.67$$

OK

Consider Second-Order Effects

$$L_b = \sqrt{h^2 + (0.5(L-e))^2} \quad \text{(From Work Points)}$$

$$L_b = 15.9 \text{ ft}$$

$$B_1 = C_m / (1 - \alpha P_r / P_{e1}) \geq 1 \quad \text{310-10 Eqn A-8-3}$$

$$\alpha = 1 \quad \text{(LRFD)}$$

$$C_m = 0.6 \quad \text{(M}_1=0\text{)}$$

$$P_r = P_u = 398 \text{ k} \quad \text{(First Order Estimate)}$$

$$P_{e1} = \pi^2 EI / (K_1 L)^2 \quad \text{310-10 Eqn A-8-5}$$

$$EI = 107541.7 \text{ k-ft}^2$$

$$K_1 = 1 \quad \text{(Assumed)}$$

$$L = 15.9 \text{ ft}$$

$$P_{e1} = 4175 \text{ k}$$

$$B_1 = 0.663 \Rightarrow 1$$

$$B_2 = 1.06$$

$$P_{nt} = 26 \text{ k} \quad M_{nt} = 4 \text{ k-ft}$$

$$P_{lt} = 371 \text{ k} \quad M_{lt} = 151 \text{ k-ft}$$

$$M_r = B_1 M_{nt} + B_2 M_{lt}$$

$$M_r = 164 \text{ k-ft}$$

$$P_r = P_{nt} + B_2 P_{lt}$$

$$P_r = 419.1633 \text{ k}$$

Check Combined Loading

$$KL_y = L_{bx} = 15.9 \text{ ft} \quad \text{W10X88}$$

$$p = 1.26 \times 10^{-3} \text{ (k-ft)}^{-1} \quad \text{360-10 T. 6-1}$$
$$b_x = 2.24 \times 10^{-3} \text{ (k-ft)}^{-1}$$

$$P_r/P_c = pP_r = 0.528 \geq 0.2$$

$$(8/9)(M_{rx}/M_{cx}) = b_x M_{rx}/R_y$$
$$b_x M_{rx} = 0.367$$

$$pP_r + B_x M_{rx} = 0.896 \quad \text{360-10 Eqn 6-1/2}$$

OK

Check Shear

$$\lambda_{sw} = 2.24 \sqrt{E/F_y}$$

$$\lambda_{sw} = 53.95$$

$$\lambda_w = 17.85$$

$$\lambda_w \leq \lambda_{sw}$$
$$\phi \text{ \& } C_v = 1.0$$

$$\phi V_n = \phi 0.6 F_y A_w C_v$$

$$\phi V_n = 196 \text{ k}$$

$$\phi V_n (\text{k}) = 196 > V_u (\text{k}) = 9$$

OK

Member 1BR OK

P_D (k)	P_L (k)	P_{QE} (k)	P_S (k)
20.9	11.5	38.8	0
V_D (k)	V_L (k)	V_{QE} (k)	V_S (k)
0.7	0.1	1.1	0
M_D (k-ft)	M_L (k-ft)	M_{QE} (k-ft)	M_S (k-ft)
3.4	2.2	16.9	0

RISA 3D Outputs

Section W10X100

d (in)	t_w (in)	A_g (in ²)	t_f (in)	e (in)	Δ_p (in)
11.1	0.68	29.3	1.12	48	0.12
b_f (in)	Z_x (in ³)	E (ksi)	F_y (ksi)	h (ft)	L (ft)
10.3	130	29000	50	12	25
I_x (in ⁴)	R_y				
623	1.1				

AISC 360-10

T. 1-1

T. 3-2

Determine Factored Loads (Based on Link Shear Overstrength)

$$V_{QE} = 26 \text{ k (Link Shear Force)}$$

$$V_n = 180 \text{ k (Link)}$$

$$1.25R_y V_n = 247 \text{ k (Amplified Link Shear Force)}$$

$$1.25R_y V_n / V_{QE} = 9.51 \text{ (Overstrength Factor)}$$

$$M_E = 161 \text{ k-ft}$$

$$P_E = 369 \text{ k (in beam due to link)}$$

$$V_E = 10 \text{ k}$$

P_u (k)	V_u (k)	M_u (k-ft)
403	11	167

From Load Calculations

Check Slenderness (Moderately Ductile)

341-10 D1

$$\lambda_f = b_f / 2t_f$$

$$\lambda_f = 4.60$$

$$\lambda_{ps} = 0.38 \sqrt{E/F_y}$$

$$\lambda_{ps} = 9.15$$

AISC 341-10

T. D1.1

$$\lambda_f = 4.60 < \lambda_{ps} = 9.15$$

OK

$$\lambda_w = d/tw$$

$$\lambda_w = 16.32$$

$$C_a = P_u / \phi_c P_y \quad \text{T. D1.1}$$

$$C_a = 0.306$$

$$\lambda_{ps} = 1.12 \sqrt{E/F_y} (2.33 - C_a) \geq 1.49 \sqrt{E/F_y} \quad \text{T. D1.1}$$

$$\lambda_{ps} = 54.60$$

$$\lambda_w = 16.32 < \lambda_{ps} = 54.60$$

OK

Consider Second-Order Effects

$$L_b = \sqrt{h^2 + (0.5(L-e))^2} \quad \text{(From Work Points)}$$

$$L_b = 15.9 \text{ ft}$$

$$B_1 = C_m / (1 - \alpha P_r / P_{e1}) \geq 1 \quad \text{310-10 Eqn A-8-3}$$

$$\alpha = 1 \quad \text{(LRFD)}$$

$$C_m = 0.6 \quad \text{(M}_1=0)$$

$$P_r = P_u = 403 \text{ k} \quad \text{(First Order Estimate)}$$

$$P_{e1} = \pi^2 EI / (K_1 L)^2 \quad \text{310-10 Eqn A-8-5}$$

$$EI = 125465.3 \text{ k-ft}^2$$

$$K_1 = 1 \quad \text{(Assumed)}$$

$$L = 15.9 \text{ ft}$$

$$P_{e1} = 4870 \text{ k}$$

$$B_1 = 0.654 \Rightarrow 1$$

$$B_2 = 1.15$$

$$P_{nt} = 34 \text{ k}$$

$$M_{nt} = 6 \text{ k-ft}$$

$$P_{lt} = 369 \text{ k}$$

$$M_{lt} = 161 \text{ k-ft}$$

$$M_r = B_1 M_{nt} + B_2 M_{lt}$$

$$P_r = P_{nt} + B_2 P_{lt}$$

$$M_r = 190 \text{ k-ft}$$

$$P_r = 456.6698 \text{ k}$$

Check Combined Loading

$$KL_y = L_{bx} = 15.9 \text{ ft} \quad \text{W10X100}$$

$$\begin{aligned} p &= 1.11 \times 10^{-3} \text{ (k-ft)}^{-1} \\ b_x &= 1.93 \times 10^{-3} \text{ (k-ft)}^{-1} \end{aligned} \quad 360-10 \text{ T. 6-1}$$

$$P_r/P_c = pP_r = 0.507 \geq 0.2$$

$$\begin{aligned} (8/9)(M_{rx}/M_{cx}) &= b_x M_{rx}/R_y \\ b_x M_{rx} &= 0.368 \end{aligned}$$

$$pP_r + B_x M_{rx} = 0.874 \quad 360-10 \text{ Eqn 6-1/2}$$

OK

Check Shear

$$\lambda_{sw} = 2.24 \sqrt{E/F_y}$$

$$\lambda_{sw} = 53.95$$

$$\lambda_w = 16.32$$

$$\begin{aligned} \lambda_w &\leq \lambda_{sw} \\ \phi &\& \text{ Cv} = 1.0 \end{aligned}$$

$$\phi V_n = \phi 0.6 F_y A_w C_v$$

$$\phi V_n = 226 \text{ k}$$

$$\phi V_n (\text{k}) = 226 > V_u (\text{k}) = 11$$

OK

Member 2C OK

P_D (k)	P_L (k)	P_{QE} (k)	P_S (k)
31.1	0	2.7	0.6
M_D (k-ft)	M_L (k-ft)	M_{QE} (k-ft)	M_S (k-ft)
0	0	0	0

RISA 3D Outputs

Section W12X96

d (in)	t_w (in)	A_g (in ²)	t_f (in)	I_x (in ⁴)	L (ft)
12.7	0.55	28.2	0.9	833	12
b_f (in)	Z_x (in ³)	E (ksi)	Fy (ksi)	R_y	
12.2	147	29000	50	1.1	

AISC 360-10
T. 1-1
T. 3-2

Determine Factored Loads

1) Redundancy Seismic Load Combinations

P_u (k)	M_u (k-ft)
44	0

From Load Calcs

2) Overstrength Seismic Load Combinations

P_u (k)
47

Moment and Shear
Analysis Not
Required

3) Strain Hardened Expected Yield Strengths

$$\Sigma V_n = 180 \text{ k} \quad (\text{All Levels Above Column Top})$$

$$1.1R_y \Sigma V_n = P_E = 218 \text{ k} \quad (\text{Not Used w/ } \rho \text{ or } \Omega \text{ in Combos})$$

P_u (k)	M_u (k-ft)
260	0

Governing Combination

P_u (k)	M_u (k-ft)
260	0

Check Slenderness (Highly Ductile)

341-10 D1

$$\lambda_f = b_f / 2t_f$$

$$\lambda_f = 6.78$$

$$\lambda_{ps} = 0.3 \sqrt{E/F_y}$$

$$\lambda_{ps} = 7.22$$

AISC 341-10

T. D1.1

$$\lambda_f = 6.78 < \lambda_{ps} = 7.22$$

OK

$$\lambda_w = (d - 2t_f) / t_w$$

$$\lambda_w = 19.82$$

$$C_a = P_u / \phi_c P_y$$

$$C_a = 0.205$$

T. D1.1

$$\lambda_{ps} = 0.77 \sqrt{E/F_y} (2.93 - C_a) \geq 1.49 \sqrt{E/F_y}$$

$$\lambda_{ps} = 50.53$$

T. D1.1

$$\lambda_w = 19.82 < \lambda_{ps} = 50.53$$

OK

Consider Second-Order Effects

$$L_b = 12.0 \text{ ft} \quad (\text{From Work Points})$$

$$B_1 = C_m / (1 - \alpha P_r / P_{e1}) \geq 1$$

310-10 Eqn A-8-3

$$\alpha = 1 \quad (\text{LRFD})$$

$$C_m = 1 \quad (M_1 = 0)$$

$$P_r = P_u = 260 \text{ k} \quad (\text{First Order Estimate})$$

$$P_{e1} = \pi^2 EI / (K_1 L)^2$$

310-10 Eqn A-8-5

$$EI = 167756.9 \text{ k-ft}^2$$

$$K_1 = 1 \quad (\text{Assumed})$$

$$L = 12.0 \text{ ft}$$

$$P_{e1} = 11498 \text{ k}$$

$$B_1 = 1.023 \Rightarrow 1.023$$

$$B_2 = 1.06$$

$$P_{nt} = 42 \text{ k}$$

$$P_{lt} = 218 \text{ k}$$

$$M_{nt} = 0 \text{ k-ft}$$

$$M_{lt} = 0 \text{ k-ft}$$

$$M_r = B_1 M_{nt} + B_2 M_{lt}$$

$$M_r = 0 \text{ k-ft}$$

$$P_r = P_{nt} + B_2 P_{lt}$$

$$P_r = 273 \text{ k}$$

Check Combined Loading

$$KL_y = L_{bx} = 12.0 \text{ ft} \quad \text{W12X96}$$

$$p = 0.924 \times 10^{-3} \text{ (k-ft)}^{-1}$$

$$b_x = 1.63 \times 10^{-3} \text{ (k-ft)}^{-1}$$

360-10 T. 6-1

$$P_r/P_c = pP_r = 0.252 \geq 0.2$$

$$(8/9)(M_{rx}/M_{cx}) = b_x M_{rx}/R_y$$

$$b_x M_{rx} = 0.000$$

$$pPr + B_x M_{rx} = 0.252$$

OK

360-10 Eqn 6-1/2

Member 1C

OK

P_D (k)	P_L (k)	P_{QE} (k)	P_S (k)
76.6	20	14.3	2
M_D (k-ft)	M_L (k-ft)	M_{QE} (k-ft)	M_S (k-ft)
0	0	0	0

RISA 3D Outputs

Section W12X96

AISC 360-10

d (in)	t_w (in)	A_g (in ²)	t_f (in)	I_x (in ⁴)	L (ft)
12.7	0.55	28.2	0.9	833	12
b_f (in)	Z_x (in ³)	E (ksi)	Fy (ksi)	R_y	
12.2	147	29000	50	1.1	

T. 1-1

T. 3-2

Determine Factored Loads

1) Redundancy Seismic Load Combinations

P_u (k)	M_u (k-ft)
132	0

From Load Calcs

2) Overstrength Seismic Load Combinations

P_u (k)
142

Moment and Shear
Analysis Not
Required

3) Strain Hardened Expected Yield Strengths

$$\Sigma V_n = 360 \text{ k} \quad (\text{All Levels Above Column Top})$$

$$1.1R_y \Sigma V_n = P_E = 435 \text{ k} \quad (\text{Not Used w/ } \rho \text{ or } \Omega \text{ in Combos})$$

P_u (k)	M_u (k-ft)
548	0

Governing Combination

P_u (k)	M_u (k-ft)
548	0

Check Slenderness (Highly Ductile)

341-10 D1

$$\lambda_f = b_f/2t_f$$

$$\lambda_f = 6.78$$

$$\lambda_{ps} = 0.3\sqrt{E/F_y}$$

$$\lambda_{ps} = 7.22$$

AISC 341-10

T. D1.1

$$\lambda_f = 6.78 < \lambda_{ps} = 7.22$$

OK

$$\lambda_w = (d-2t_f)/t_w$$

$$\lambda_w = 19.82$$

$$C_a = P_u/\phi_c P_y$$

$$C_a = 0.432$$

T. D1.1

$$\lambda_{ps} = 0.77\sqrt{E/F_y}(2.93 - C_a) \geq 1.49\sqrt{E/F_y}$$

$$\lambda_{ps} = 46.33$$

T. D1.1

$$\lambda_w = 19.82 < \lambda_{ps} = 46.33$$

OK

Consider Second-Order Effects

$$L_b = 12.0 \text{ ft} \quad (\text{From Work Points})$$

$$B_1 = C_m/(1 - \alpha P_r/P_{e1}) \geq 1$$

310-10 Eqn A-8-3

$$\alpha = 1 \quad (\text{LRFD})$$

$$C_m = 1 \quad (M_1=0)$$

$$P_r = P_u = 548 \text{ k} \quad (\text{First Order Estimate})$$

$$P_{e1} = \pi^2 EI / (K_1 L)^2$$

310-10 Eqn A-8-5

$$EI = 167756.9 \text{ k-ft}^2$$

$$K_1 = 1 \quad (\text{Assumed})$$

$$L = 12.0 \text{ ft}$$

$$P_{e1} = 11498 \text{ k}$$

$$B_1 = 1.050 \Rightarrow 1.050$$

$$B_2 = 1.15$$

$$P_{nt} = 113 \text{ k} \quad M_{nt} = 0 \text{ k-ft}$$

$$P_{lt} = 435 \text{ k} \quad M_{lt} = 0 \text{ k-ft}$$

$$M_r = B_1 M_{nt} + B_2 M_{lt}$$

$$M_r = 0 \text{ k-ft}$$

$$P_r = P_{nt} + B_2 P_{lt}$$

$$P_r = 611 \text{ k}$$

Check Combined Loading

$$KL_y = L_{bx} = 12.0 \text{ ft} \quad \text{W12X96}$$

$$p = 0.924 \times 10^{-3} \text{ (k-ft)}^{-1} \quad \text{360-10 T. 6-1}$$

$$b_x = 1.63 \times 10^{-3} \text{ (k-ft)}^{-1}$$

$$P_r/P_c = pP_r = 0.565 \geq 0.2$$

$$(8/9)(M_{rx}/M_{cx}) = b_x M_{rx}/R_y$$

$$b_x M_{rx} = 0.000$$

$$pP_r + B_x M_{rx} = 0.565 \quad \text{360-10 Eqn 6-1/2}$$

$$\text{OK}$$